A HIGH CMRR INSTRUMENTATION AMPLIFIER FOR BIOPOTENTIAL SIGNAL ACQUISITION

A Thesis

by

Reza Muhammad Abdullah

Submitted to the Office of Graduate Studies of
Texas A&M University
in partial fulfillment of the requirements for the degree of

MASTER OF SCIENCE

May 2011

Major Subject: Electrical Engineering

A HIGH CMRR INSTRUMENTATION AMPLIFIER FOR BIOPOTENTIAL SIGNAL ACQUISITION

A Thesis

by

Reza Muhammad Abdullah

Submitted to the Office of Graduate Studies of
Texas A&M University
in partial fulfillment of the requirements for the degree of

MASTER OF SCIENCE

Approved by:

Chair of Committee,	Edgar Sanchez-Sinencio
Committee Members,	Hamid A. Toliyat
	Samuel Palermo
	Duncan Henry M. Walker
Head of Department,	Costas N. Georghiades

May 2011

Major Subject: Electrical Engineering

ABSTRACT

A High CMRR Instrumentation Amplifier for Biopotential
Signal Acquisition. (May 2011)
Reza Muhammad Abdullah, B.Sc., Kwame Nkrumah University of Science & Tech
Chair of Advisory Committee: Dr. Edgar Sanchez-Sinencio

Biopotential signals are important to physicians for diagnosing medical conditions in patients. Traditionally, biopotentials are acquired using contact electrodes together with instrumentation amplifiers (INAs). The biopotentials are generally weak and in the presence of stronger common mode signals. The INA thus needs to have very good Common Mode Rejection Ratio (CMRR) to amplify the weak biopotential while rejecting the stronger common mode interferers. Opamp based INAs with a resistor-capacitor feedback are suitable for acquiring biopotentials with low power and low noise performance. However, CMRR of such INA topologies is typically very poor.

In the presented research, a technique is proposed for improving the CMRR of opamp based INAs in RC feedback configurations by dynamically matching input and feedback capacitor pairs. Two instrumentation amplifiers (one fully differential and the other fully balanced fully symmetric) are designed with the proposed dynamic element matching scheme.

Post layout simulation results show that with 1% mismatch between the limiting capacitor pairs, CMRR is improved to above 150dB when the proposed dynamic element matching scheme is used. The INAs draw about 10uA of quiescent current from a 1.5 dual power supply source. The input referred noise of the INAs is less than $3uV/\sqrt{Hz}$.

ACKNOWLEDGEMENTS

First, I would like to thank my committee chair, Dr. Edgar Sanchez-Sinencio for his expert guidance and for encouragement he gave me during the time I have spent pursuing a Master's degree at Texas A&M University. My thanks also goes to my committee members and all the professors in the Analog & Mixed Signal Center of Texas A&M University for all the technical support I have received during my stay as part of the group. I also extend my gratitude to Texas Instruments Incorporated for initiating the AAURP (African Analog University Relations Program) initiative through which I was introduced to Analog Integrated Circuits. My thanks also go to Texas Instruments for sponsoring my Master's education here at Texas A&M University. To my fellow colleagues and office mates of the Analog and Mixed Signal Center (AMSC), thank you for all the help and understanding shown to me at all times. Finally, I want to acknowledge my parents, siblings and all family members who have in numerous ways supported and encouraged me throughout my pursuit of Electrical Engineering as a profession. Thank you all.

TABLE OF CONTENTS

Page

LIST OF FIGURES

FIGURE Page

LIST OF TABLES

1. INTRODUCTION

The importance of bio-potential signals to physicians for diagnosing medical conditions and also general in-patient/ out patient monitoring cannot be overestimated. Electrocardiogram (EKG) signals - that is the bio-potential signal that results from internal electrochemical processes within the heart – can be used to monitor a patients' health condition. Electroencephalogram (EEG) and EMG (Electromyogram) respectively are electrical signals resulting from the human brain activity and from contraction/ relaxation of body muscles.

Traditionally, these signals are acquired using electrodes and amplified using instrumentation amplifiers. Acquisition of these signals is done differentially while any common mode component of the bio-potential is rejected. This is very essential because the required bio-potentials are typically weak signals with low voltage levels where as the likely common mode signals that are coupled with the bio-potentials are much larger in amplitude. For instance, in EKG acquisition, signal amplitudes are typically in micro-volt range with maximum values about 0.5mV. A 60Hz interference signal from the supply mains is typically coupled to the differential electrodes and thus appears as a common signal which is much larger in voltage compared to the desired EKG signal. This signal is referred to as a common mode signal and has to be rejected where as the differential EKG signals is acquired.

The ability of an instrumentation amplifier to amplify required differential signals while rejecting unwanted common mode signals is quantified by its Common Mode Rejection Ratio (CMRR). Instrumentation amplifier properties vary depending on its topology and application.

This thesis follows the style of the IEEE Journal of Solid-State Circuits.

The most common instrumentation amplifier is the 3 - Opamp instrumentation amplifier. This topology though is not suitable for portable bio-potential signal monitoring since it demands high power consumption and has very poor CMRR. The poor CMRR of the 3-Opamp IA is due to the use of passive components in its feedback network. The CMRR depends on the mismatch of these passive components and degrades very quickly with slight percentage mismatch in these components.

Various Instrumentation amplifiers have been proposed for purposes of bio-potential signal acquisition targeting low power, low noise and high CMRR specifications. Single Opamp topologies such as [1] have the advantage of lower power consumption however the problem of poor CMRR is not addressed. Current feedback topologies as in [2] and [3] have better CMRR however the inaccuracy of the gain of such topologies makes design of these amplifiers a little complex.

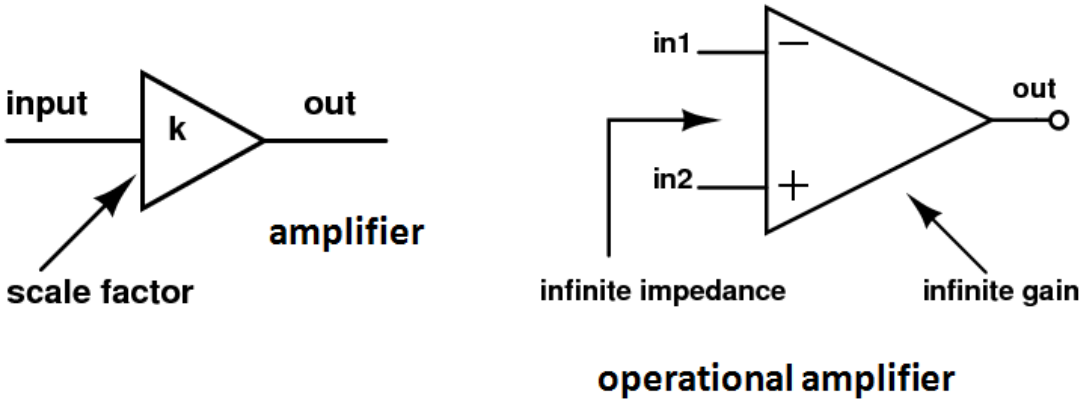

Figure 1-1 Block Diagram of an Amplifier and Operational Amplifier

A. Amplifiers, Operational Amplifiers and Instrumentation Amplifiers

The operational amplifier (opamp) is one of the most common circuits used in analog electronic circuit design. Its uses are very wide and opamps are found in sorts of applications from power management systems to RF circuits and data converters. As an

ideal black box, the opamps magnifies the voltage difference between its inputs by several orders. In more specific terms, the ideal opamp has infinite gain, with infinite input impedance and zero output impedance. These properties are desirable in all applications where opamps are used.

An amplifier is somewhat of a loose term implying any system or block that produces an output quantity that is a scaled version of its input. The input could be a single ended signal or the difference of two signals. More commonly, the output of an amplifier is a scaled current or voltage. Current and voltage amplifiers can be built using opamps in negative feedback configurations or using entirely different circuit topologies. Figure 1-1 shows the block diagrams of amplifiers and operational amplifiers.

Table 1-1 Properties of INAs vs. Opamps

Properties	**Opamp**	**INA**
Gain	Very Large	Finite
Gain Accuracy	High	Very High
CMRR	High	Very High
`Noise	Low	Very Low`

Instrumentation Amplifiers (INAs) are special amplifiers designed where long term accuracy and stability of the amplifier is desired. They are difference amplifiers in that they have two inputs, the difference of which is amplified to produce the desired output. Most instrumentation amplifiers will have at least one opamp and some negative feedback network to produce the desired fixed gain. However, it should be noted that there are a few open loop INA topologies as well. INAs typically have very good

common mode rejection ratio (CMRR) and high input impedances. Table 1-1 shows the general properties of opamps versus instrumentation amplifiers.

B. Applications of Instrumentation Amplifiers

The characteristics of instrumentation amplifiers mentioned in the previous section make them very suitable for Measurement and Test applications. Besides that they are used in a host of sensor applications such as temperature and pressure sensing. INAs are also used in biomedical fields. A typical example of such use is in the front end of biopotential acquisition systems. Figure 1-2 shows four major application areas of instrumentation amplifiers.

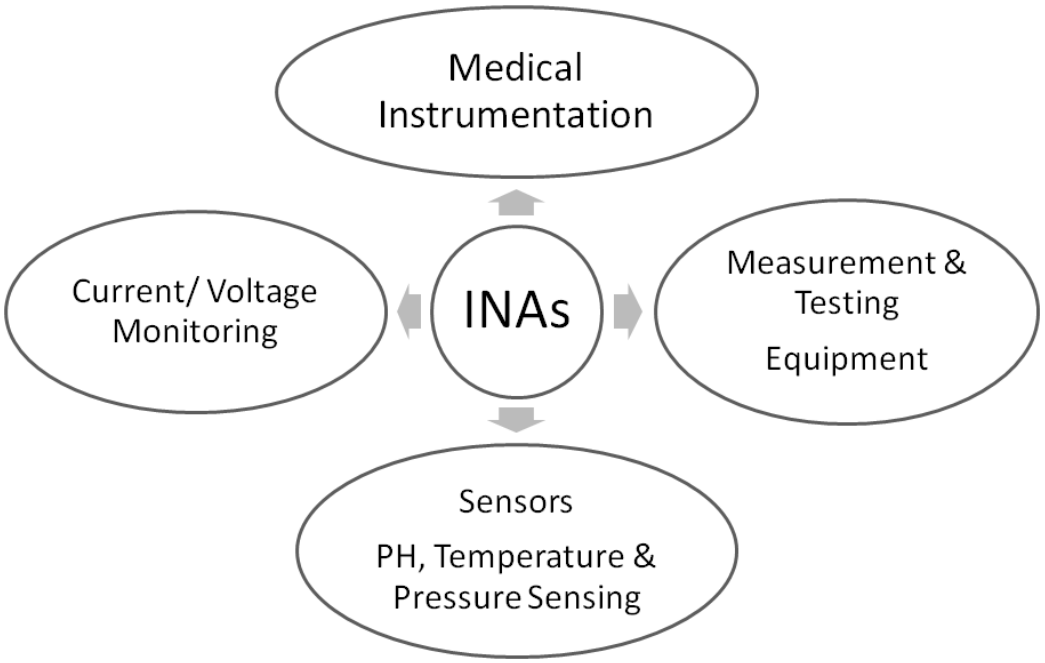

Figure 1-2 Applications of Instrumentation Amplifiers

For this research effort, we focus on using instrumentation amplifiers for acquiring biopotential signals. Such instrumentation amplifiers are also known as biopotential signal amplifiers.

1. Biopotential Signal Acquisition

Biopotentials are very important to physicians in modern medical practice. These are electrical signals generated as a result of electro-chemical processes that occur within the human body. The kind of body cells involved in these electro-chemical processes determine what biopotential signal is generated and its possible use to physicians. The most common biopotentials are electroencephalogram (EEG), electrocardiogram (EKG) and electromyogram (EMG). Electroencephalogram (EEG) is generated as a result of neuron activity within the brain, EMG due to electrical activity of skeletal muscles and EKG as a result of electrical impulses that are generated due to the pumping activity of the heart.

The above mentioned biopotentials are generated due to combination of *action potentials* from several cells associated with the tissue/ organ [4]. Each action potential is a cycle of potential changes across the cell membrane. During a cells inactive state, its exhibits a potential referred to as a *resting potential.* In this state, the membrane of the cell is more permeable to K+ than Na+. As such, K+ has higher concentration within the cell in their inactive state. This diffusion gradient across the cell membrane causes K+ ions to slowly move across the membrane to the exterior, making the interior more negative with respect to the exterior of the cell membrane, and thus building an electric field in the process. This continues until equilibrium point when the electric field balances the K+ diffusion gradient. The voltage build up at this point is about 70mV. Any electrical stimulation of the cell at this point makes it more permeable to Na+ and these Na+ ions diffuse into the cell reducing the electric field to about 40mV. The cell membrane becomes even more permeable to K+ at this point resulting in sharp diffusion of K+ into the cell again until the electric field drops to zero volts thus returning the cell to its resting potential. It is this cycle of events that is referred to as the action potential of a cell [4].

The different biopotentials have unique electrical characteristics which need to be considered carefully when acquiring the signal. Most basic are the frequency range and amplitude levels of the signal.

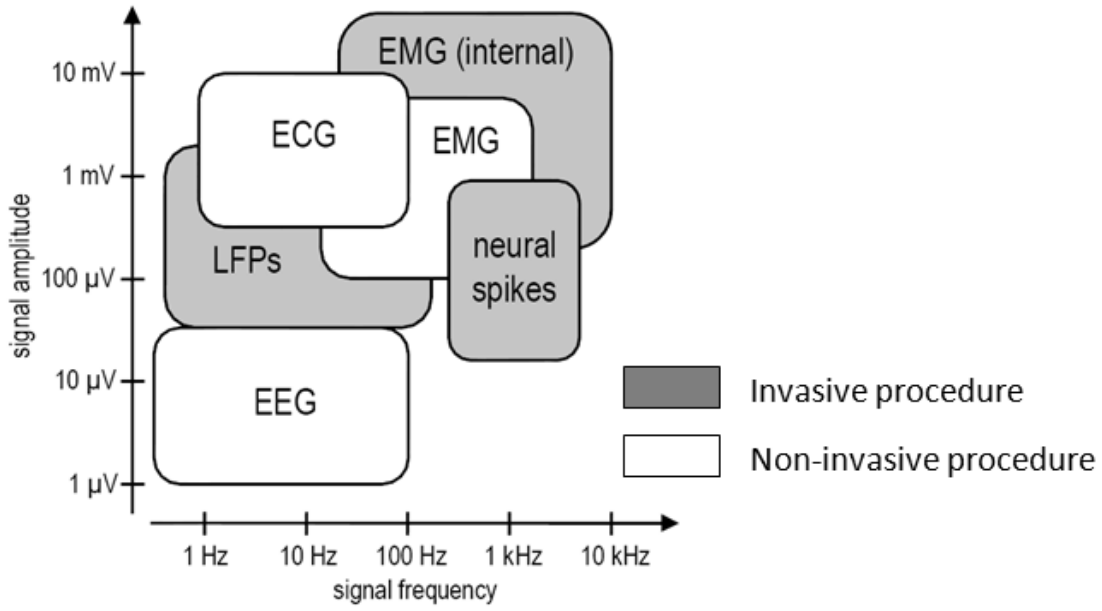

Figure 1-3 Amplitude and Frequency Characteristics of Some Biopotentials [1]

The spectrum of an EKG signal is mostly concentrated within 0.5 Hz to 150 Hz frequency range. The amplitudes of EKG (ECG) signals vary from a low of 0.5mV to a high of approximately 10mV. Figure 1-3 shows the amplitude and frequency characteristics of some other biopotential signals. Note that the biopotentials in the dark shaded boxes are acquired using invasive procedures. This will be mentioned in the next section. LFPs (Local Field Potentials) are biopotentials obtained from the dendrons of neural cells within the brain. EEG (Electroencephalogram) and EMG (Electromyogram) are the result of electrochemical activity within the brain and skeletal muscle tissue respectively.

1.1. Model for Biopotential Electrodes

Biopotentials can be acquired invasively or non-invasively using electrodes. The electrode is an interface between the body and the input of the instrumentation amplifier or readout circuitry. This interface (transducer) is necessary because current conduction in the body is a result of ionic movement whereas in the readout front end it is a result of electron motion. The electrode is thus a metal – electrolyte interface. In simple terms a chemical reaction occurs when the metal comes in contact with a specific electrolyte and this reaction results in the generation of free electrons (an oxidation reaction). This unsettles the neutrality of the metal – electrolyte interface and creates an electron gradient across it resulting in current flow.

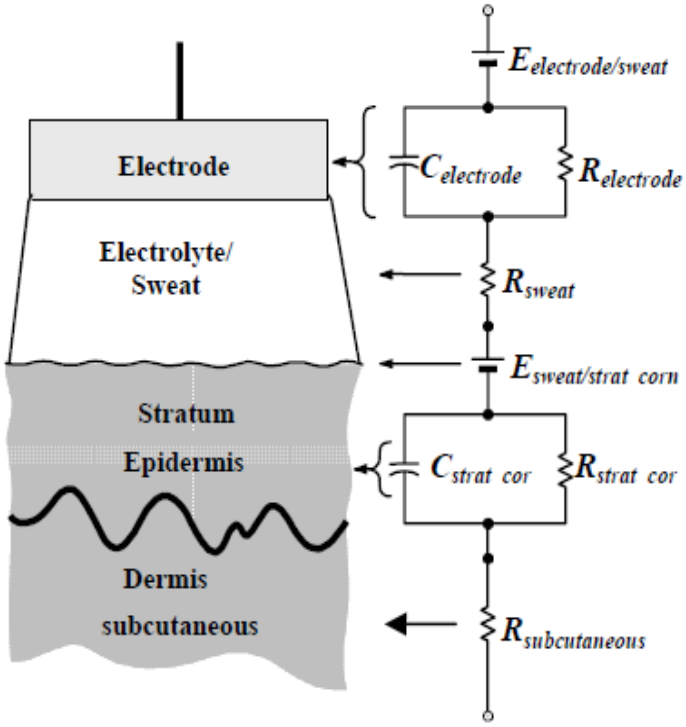

Figure 1-4 Electrical Model for Skin - Electrode Interface [4]

Electrodes could be wet, dry or non-contact electrodes. Wet electrodes usually have a gel like substance that creates contact between the body and the electrode. These types are

the most common and Ag/ AgCl in particular are in wide use. Dry electrodes do away with the gel like substance thus the contact resistance at the body – electrode interface is quite high. However these are more comfortable to use. Finally, non – contact electrode no physical contact with the body and behave capacitively. In Figure 1-4 is the structure and a linear electrical model for the skin – electrode interface. Actually in this model, two interfaces are shown. First is the skin – sweat interface which is modeled as a resistor in series with a capacitor – resistor parallel combination that includes a dc offset voltage. The second is the interface between the sweat and the biopotential electrode. Typical values of the R's and C's are shown in Tables 1-2 and 1-3.

Table 1-2 Electrical Characteristics of Commonly Used Electrodes

Electrode	**Offset**	**Resistance**	**Capacitance**
Ag/AgCl	0.1 – 50mV	1 – 10k ohms	100 – 150nF
Stainless Steel	1 – 50mV	3 – 12k ohms	< = 100nF

Table 1-3 Typical Skin Impedance Parameters

Impedance	**Prepared Skin**	**Unprepared Skin**
Subcutaneous Resistance	< = 120 ohms	< = 120 ohms
Stratum Resistance	Up to 100k ohms	1 – 2 M ohms
Shunt Capacitance	Up to 10nF	Up to 40nF

1.2. Biopotential Amplifiers

The biopotential amplifier [5],[6] is the main block that amplifiers the weak biopotential signals to levels that can be analyzed and used by physicians. The biopotential amplifier however has to meet certain criteria so as not to corrupt the signal during the acquisition process. It has been mentioned earlier in the previous sections that the biopotentials have an embedded dc offset due to the difference in the half cell potentials of the electrodes used to acquire the signal. The dc offset, also referred to as the *Differential Electrode Offset (DEO)*, has to be filtered out before or during the acquisition process to avoid saturating the biopotential amplifier. Also, the amplifier should be able to selectively amplify only the biopotential signal of interest while attenuating signals of any other frequency. In other words, the biopotential amplifier should have frequency characteristics suitable for kind of biopotential that is being acquired.

Also, since the biopotentials themselves are very weak signals, the input referred noise of the biopotential amplifier should be very small to make the biopotentials detectable by the acquisition system. Low noise of the biopotential amplifier is very critical. One more very pertinent issue to be considered when designing instrumentation amplifiers is interference from unwanted sources.

Electromagnetic and electrostatic interference from the mains of buildings are sources of unwanted signals for biopotential acquisition systems [4]. Whenever an alternating current flows through a conductor, an electromagnetic field (EM field) is generated around the conductor, and when this EM field cuts across the loop of conductors and electromotive force (EMF) is generated. This is the principle of operation of a generator. A similar effect occurs when the mains current of a building generates an EM field and this field in turn cuts through the loop formed by the human body, the leads between the electrodes and the input of the biopotential amplifier, and the biopotential amplifier itself. Thus an unwanted AC signal is generated that is common to both inputs of the biopotential amplifier.

On the other hand, unwanted interference can be due to electrostatic effects and this is explained using the Figure 1-5. C_{bp} is the capacitance between mains and the human body while C_{bg} is the capacitance between the body and ground. C_{ISO} is the capacitance between the circuit ground the earth. R_{e1} and R_{e2} are the resistances of the circuit leads. A displacement current, I_D, flows into the body through these capacitances and splits about equally between the isolation capacitance and the body to ground capacitance. The voltage created as a result of this current and the ground resistance appears as a common mode signal at the inputs of the biopotential amplifier.

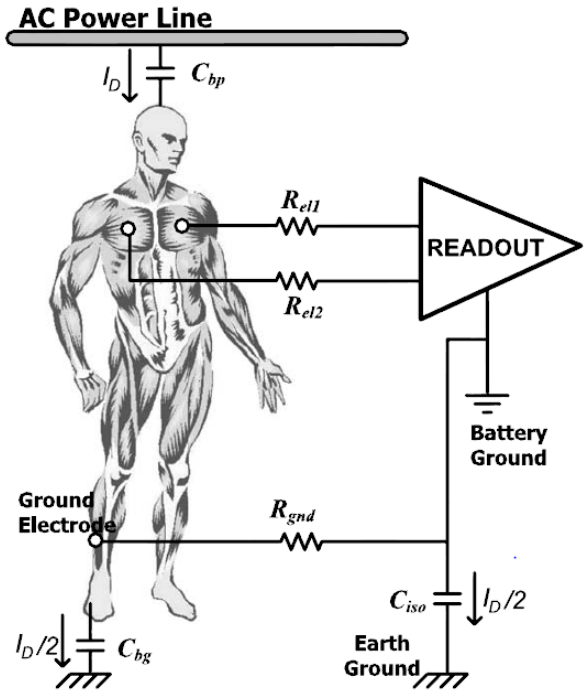

Figure 1-5 Electrostatic Interference to Human Body [4]

Since the unwanted signals due to EMI and ESI are common mode, the biopotential amplifier needs to have very good Common Mode Rejection properties. Common Mode Rejection Ratio (CMRR) is therefore another very critical parameter for biopotential amplifier.

Besides these main critical specifications for the biopotential amplifier, power consumption has to also be minimized for the acquisition system and this begins with designing a low power biopotential amplifier. Also, to make the system more versatile, it helps to design a biopotential amplifier that is reconfigurable for varying the gain and frequency characteristics of the overall acquisition system.

In Table 1-4 are the EKG general requirements of a biopotential amplifier. The targeted application is EKG acquisition. The specifications in this table are obtained from published papers [1-3] in EKG amplifiers.

Table 1-4 General Requirements of an EKG Amplifier

Parameter	**General Specification**
CMRR	70 dB
Input Referred Noise	2-3μV rms
Input Impedance	> 5Mohm
Bandwidth	0.1 – 150 Hz
Gain	40 dB

C. Classes of Instrumentation Amplifiers

There are many ways to implement instrumentation amplifiers [1-3],[7-10] to achieve long term stability and efficiency. In general terms, we can classify most topologies under the following 2 types.

- Opamp based INAs
- Current Balancing INAs

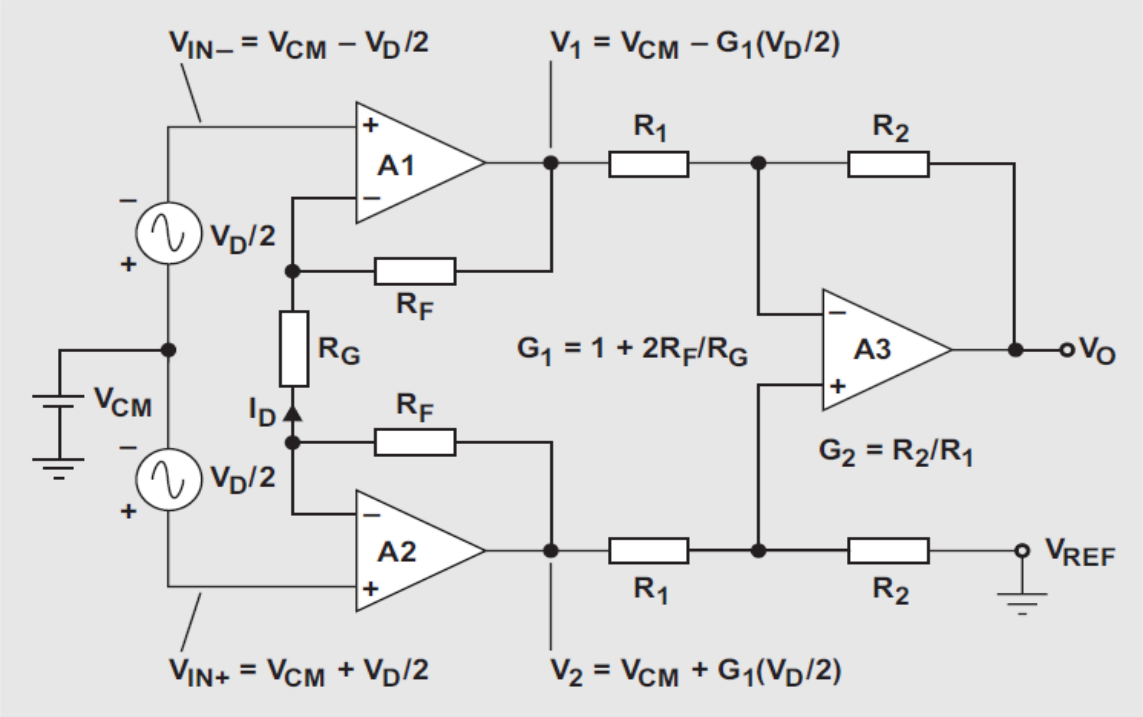

Figure 1-6 Three Opamp Instrumentation Amplifier [11]

1. Opamp Based Instrumentation Amplifiers

Opamp based INAs, as the name implies, utilize opamps and feedback networks for amplification and frequency shaping if necessary. The most common INA topology of this kind is the 3-opamp instrumentation amplifier. This is shown in Fig 1-6.

The 3 opamp INA has two stages. The overall gain of the INA is split between the two stages. In Figure 1-6, the two gain stages amplify the differential input signal by G_1 and G_2 respectively.

$$G_1 = \frac{v_1}{v_d} = 1 + \frac{2R_F}{R_G} \quad \ldots\ldots\ldots\ldots\ldots\ldots\ldots\ldots\ldots\ldots\ldots\ldots(1.1)$$

$$G_2 = \frac{v_o}{v_1} = \frac{R_2}{R_1} \quad \ldots\ldots\ldots\ldots\ldots\ldots\ldots\ldots\ldots\ldots\ldots\ldots\ldots\ldots(1.2)$$

$$G_{total} = G_1 G_2 = \frac{R_2}{R_1}\left(1 + \frac{2R_f}{R_G}\right) \quad \ldots\ldots\ldots\ldots\ldots\ldots\ldots\ldots\ldots..(1.3)$$

Typically, the 2nd stage is a unity gain stage and is only used as a difference amplifier. In the first stage, common mode signal is transferred unaltered to the inputs of the 2nd stage difference amplifier. Ideally, this scenario would mean the INA has very good rejection of common mode signals. However, the CMRR of this topology ultimately depends on the proper matching of the passive components, resistors in this case. Assuming 40dB differential gain, the resistors have to be matched to within 0.1% of each other to achieve 100dB of CMRR (Common Mode Rejection Ratio). Let $\Delta R = R_f - R_G$ and A_c = common mode gain. Then

$$A_c \approx \frac{\Delta R}{R_f + R_G} \quad \ldots\ldots\ldots\ldots\ldots\ldots\ldots\ldots\ldots\ldots\ldots\ldots\ldots..\ldots(1.4)$$

Laser trimming is required to obtain decent CMRR using this topology. Besides, the use of 3 opamps in this topology makes it a high power consuming topology and unsuitable for low power application such as portable biopotential signal acquisition systems.

2. Current Balancing Instrumentation Amplifiers

INAs of this topology can best be explained by the simplified diagram in Figure 1-7. The input stage is a transconductance stage while the output is a transimpedance. The input voltage appears across the input resistance and generates a current through it. By some means, (examples of which will be discussed in the following section), this current is mirrored into the output stage and flows through the output resistor and in the process generating the output voltage signal. Thus under ideal conditions, the gain of this INA is defined by the ratio of output to input resistors and the CMRR is independent of the matching between these resistors.

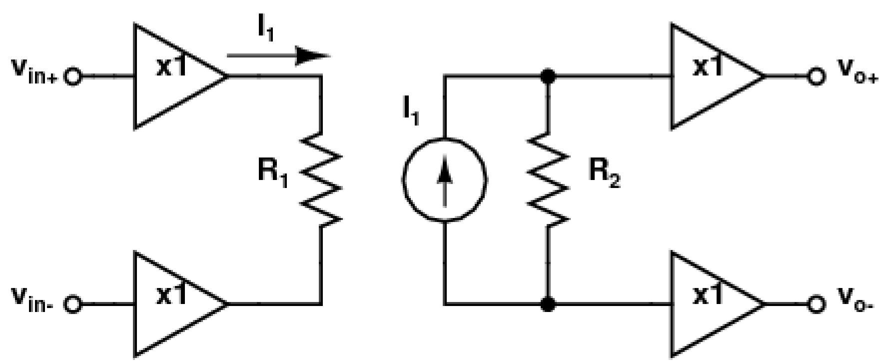

Figure 1-7 Concept of Current Balancing INA

The CBIA (Current Balancing Instrumentation Amplifier) concept seems very simple however the issue is how to copy the current from the input to output stage.

$$Av_I = \text{Gain (ideal)} = \frac{R_2}{R_1} \quad \text{......................................(1.5)}$$

The ideal case assumes that the buffers have no output resistance and that the current source is ideal. A more accurate representation of the concept is shown in Figure 1-8.

In this case the output resistances of the buffers are accounted for as well as the finite output resistance of the current source.

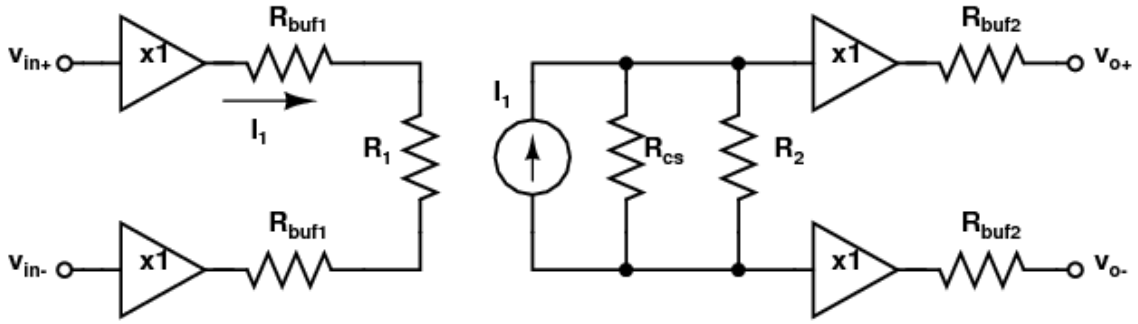

Figure 1-8 More Accurate Representation of Current Balancing INA

The gain is defined as shown in equation 1.6.

$$Av_a = \text{Gain (actual)} = \Delta . \frac{R_2}{R_1} \quad \ldots\ldots\ldots\ldots\ldots\ldots\ldots \quad (1.6)$$

$$\text{where} \qquad \Delta = \frac{R_{cs} R_1}{(R_1 + 2R_{buf})(R_2 + R_{cs})} \quad \ldots\ldots\ldots\ldots\ldots\ldots\ldots..\ldots (1.7)$$

Design & simulation of some CBIA topologies shows that the gain accuracy is usually not good because exact mirrors of the input stage current are difficult to replicate in the transimpedance output stage. In equation 1.7, Δ is some fraction less than 1. Δ approaches 1 under ideal conditions when R_{buf} is zero and R_{cs} is infinite. The design procedure of the CBIA is also more complex than that of the opamp based INA topologies. Examples of CBIAs are reported in [2],[3].

2. CMRR OF INSTRUMENTATION AMPLIFIERS

Common Mode Rejection Ratio (CMRR) is an important specification for all amplifiers with differential inputs including both single ended and fully differential output versions. For amplifiers with single ended outputs, CMRR is the ratio of the differential gain of the amplifier to the common mode gain of the amplifier. The differential gain of the amplifier is defined as the gain when differential inputs are applied whereas the common mode gain of the amplifier is the gain of the amplifier when a common signal is applied to the two inputs.

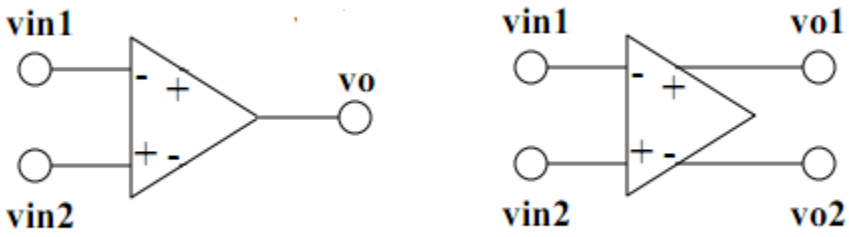

Figure 2-1 Block Diagram of Single Ended and Fully Differential Amplifiers

For fully differential amplifiers, there are two definitions of CMRR and both of them are important depending on the application of the amplifier. Figure 2-1 is a generic block diagram of a single ended and a fully differential amplifier. The CMRR for these amplifiers are defined in the next section.

A. Definition of CMRR

Let the common mode input and output voltages of the amplifiers be defined as below.

$$v_c = \frac{v_{in1} + v_{in2}}{2} \quad \text{.....(2.1a)}$$

$$v_d = \frac{v_{in1} - v_{in2}}{2} \quad \text{.....(2.1b)}$$

$$v_{od} = \frac{v_{o1} - v_{o2}}{2} \quad \text{.....(2.1c)}$$

$$v_{oc} = \frac{v_{o1} + v_{o2}}{2} \quad \text{.....(2.1d)}$$

Using the definitions in equations 2.1a to 2.1d, the common mode rejection ratio of a single ended and fully differential amplifiers are defined as in equations 2.2 and 2.3.

Single Ended Amplifier

$$\text{CMRR} = \frac{A_d}{A_c} \qquad \text{where } A_d = \frac{v_o}{v_d} \text{ and } A_c = \frac{v_o}{v_c} \quad \text{.....(2.2)}$$

Fully Differential Amplifier

$$\text{CMRR} = \frac{A_d}{A_{cc}} \qquad \text{where } A_d = \frac{v_{od}}{v_d} \text{ and } A_{cc} = \frac{v_{oc}}{v_c} \quad \text{.....(2.3)}$$

Notice the definition for the common mode gain A_{cc} of a fully differential amplifier. It is defined as the ratio of the common mode output voltage of the amplifier, to the applied common mode input signal. A_{cc} needs to be high to minimize the transfer of common mode input signal to the next stages of the biopotential acquisition system.

For EKG acquisition systems, CMRR required is at least 60dBs but state of the art biopotential INAs have typical CMRRs between 60dB and 80dB with a few topologies (mostly current balancing INA topologies) achieving CMRRs in the 100dB range. The last mentioned INAs are more complex to design however. This large CMRR specification is necessary to reject unwanted interferer signals which appear as common mode signals at the input of the biopotential INA.

B. CMRR Case Study

Consider the feedback amplifier shown in Figure 2-2. It can be used for biopotential acquisition when modified slightly.

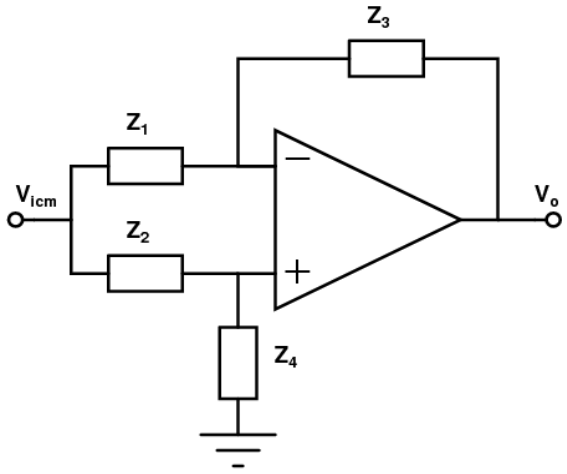

Figure 2-2 Opamp with General Impedance Feedback Configuration

1. CMRR Analysis of General Feedback Amplifier

For this analysis, we assume an ideal opamp therefore

$$A_0 \rightarrow \infty \text{ and } vn = vp$$

Performing nodal analysis on the circuit gives

$$vp(Y_2 + Y_4) - Y_2 V_{icm} = 0$$

$$vn(Y_1 + Y_3) - Y_1 V_{icm} - Y_3 V_o = 0$$

Solving the equations gives

$$A_{cm} = \frac{V_o}{V_{icm}} = \frac{Y_2 Y_3 - Y_1 Y_4}{Y_3(Y_2 + Y_4)} \quad \text{.....(2.4)}$$

Under matched impedance conditions, $Y_1 = Y_2$ and $Y_3 = Y_4$ thus common mode gain is zero and CMRR is infinite.

To account for impedance mismatch in this analysis the following assumptions are made.

$$Y_2 = Y_1 + \Delta Y_1$$

$$Y_3 = Y_4 + \Delta Y_4$$

Substituting the two above equations into (2.4) gives

$$A_{cm} = \frac{Y_1 \Delta Y_4 + Y_4 \Delta Y_1 + (\Delta Y_1)(\Delta Y_2)}{Y_1 Y_4 + Y_1 \Delta Y_4 + Y_4 \Delta Y_1 + (\Delta Y_1)(\Delta Y_2) + Y_4^2 + Y_4 \Delta Y_4} \quad \text{.....(2.5)}$$

Assume zero mismatch between Z_3 and Z_4, then $\Delta Y_4 = 0$. Simplifying (2.5) further gives

$$A_{cm}|_{\Delta Y_4=0} = \frac{\Delta Y_1}{Y_1+Y_4+\Delta Y_1} \quad \text{.....(2.6)}$$

It is observed that the common mode gain when Z_3 and Z_4 are perfectly matched is directly proportional to the amount of mismatch between impedances Z_1 and Z_2.

For the other scenario we assume zero mismatch between Z_1 and Z_2, then $\Delta Y_1 = 0$. Then

$$A_{cm}|_{\Delta Y_1=0} = \frac{Y_1\Delta Y_4}{(Y_1+Y_4)(Y_4+\Delta Y_4)} \quad \text{.....(2.7)}$$

Similar to the previous scenario, common mode gain is proportional to the mismatch between Z_3 and Z_4.

The analysis shows that under perfect impedance matching conditions, the common mode gain of the general impedance feedback amplifier is zero. However, any mismatch between the impedance worsens the common mode gain of the system in a manner that is directly proportional to the amount of mismatch in the impedances.

Figures 2-3 and 2-4 are graphs of common mode gain versus percentage of mismatch in the admittance for the cases shown in equations 2.6 and 2.7. A nominal 1 kohm resistor is assumed implying a nominal admittance of 0.001/ohm. Percentage mismatch is defined as $\Delta Y/Y$.

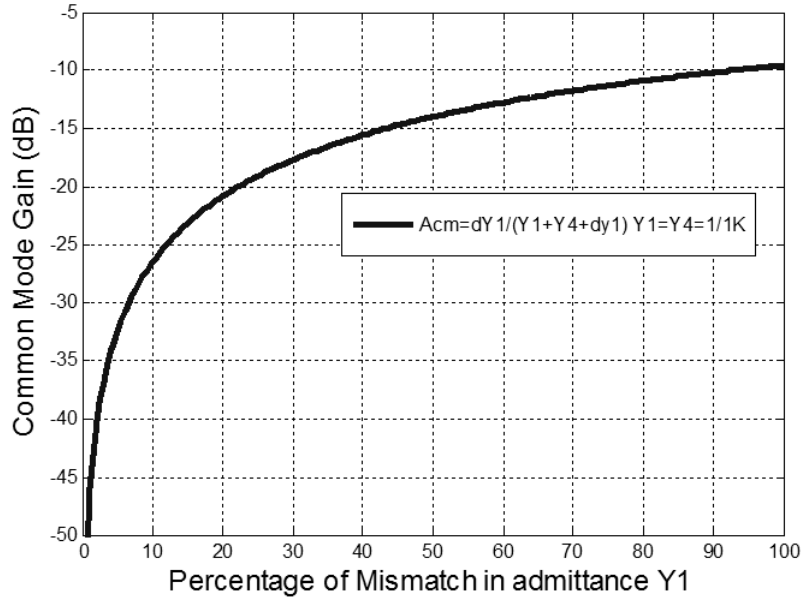

Figure 2-3 Common Mode Gain vs. Percentage Mismatch in Y1

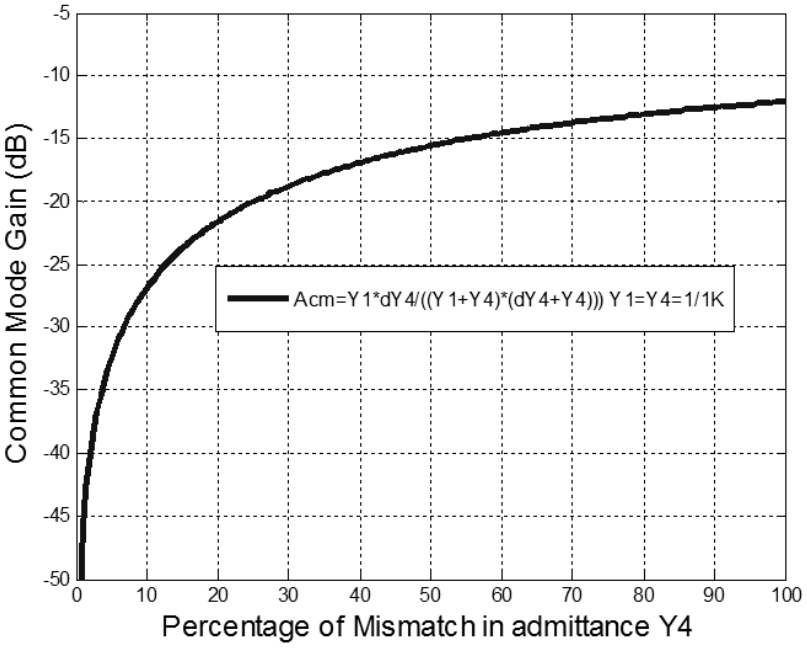

Figure 2-4 Common Mode Gain vs. Percentage Mismatch in Y4

2. CMRR Analysis of Special Case Amplifier

The feedback amplifier of Figure 2-2 can be modified and used as a simple low power biopotential INA as shown Figure 2-5. This amplifier and feedback configuration can be used for biopotential signal acquisition as will be shown at the end of this section.

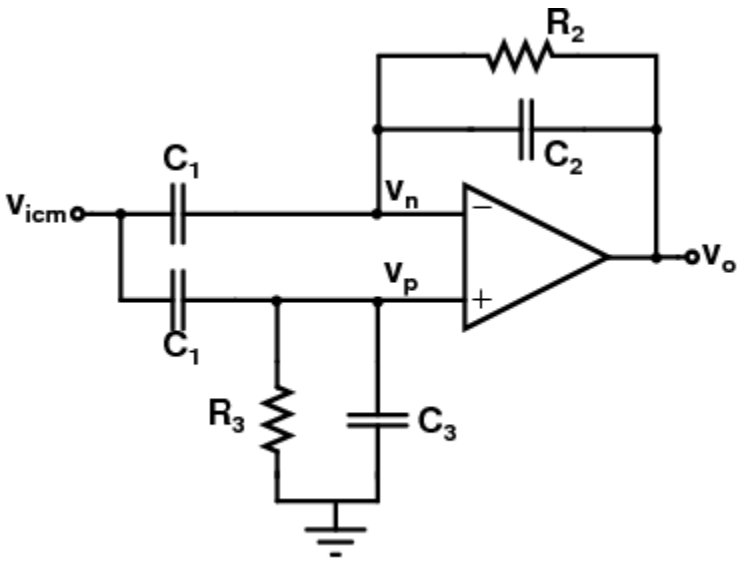

Figure 2-5 RC Feedback Amplifier Used for EKG Signal Acquisition

CMRR analysis is performed for this amplifier in the next.

As in the previous analysis, we first establish the nodal equations for the circuit in Figure 2-5.

$$vn(s(C_1 + C_2) + G) - V_o(G + sC_2) = sC_1V_{icm}$$

$$vp(s(C_1 + C_3) + G_2) - V_{icm}\,sC_1 = 0$$

Further simplification of the nodal equations and while accounting for the Δ differences in the capacitors and resistors results in common mode gain expression shown in equation 2.8.

$$A_{cm} = \frac{V_o}{V_{icm}} = \frac{s\Delta C + \Delta G}{G(G + \Delta G)} \cdot \frac{sC_1}{\left(1 + s\frac{C_1 + C_2 + \Delta C}{G + \Delta G}\right)} \cdot \frac{1}{1 + s\,{}^{C_2}/_{G}} \quad \text{.....(2.8)}$$

'G' in the nodal equations refers to the reciprocal of the resistance R_2 (conductance of R_2). For mismatch assume ΔC difference between C_2 and C_3. Also, ΔG is the difference between the conductances of R_2 and R_3.

Equation 2.8 shows that the common mode gain of this amplifier is directly proportional to the mismatch between resistor pairs and capacitor pairs. Thus we come to the same conclusion that the common mode gain worsens with increasing amount of mismatch passive element mismatch.

C. Capacitive vs. Resistive Mismatch of RC Feedback Amplifiers

For biopotential signal acquisition applications, the mismatch between the capacitors usually limits the CMRR of the INA. This is easily understood by re-examining equation 2.8. Consider the typical INA specifications for biopotential amplifiers. A typical example is shown in Table 2-1 for EKG applications.

Table 2-1 Typical Requirements of an EKG Signal Amplifier

Bandwidth	0.5 – 150 Hz
Gain	40 dB

To design an amplifier using the topology of Figure 2-3 that meets the requirements in Table 2-1, we use the capacitor and resistor values shown in Table 2-2. The procedure for obtaining these capacitor and resistor values is shown later in this thesis work.

Table 2-2 Typical Resistor and Capacitor Values for an EKG Amplifier

$\mathbf{C_1}$	20pF
$\mathbf{C_2}$	200fF
$\mathbf{R_2}$	1.0Tohm

For $\Delta = 1\%$ and at in band frequencies, say 50Hz, $s\Delta C = 2\pi \times 10^{-11}$ and $\Delta G = 1 \times 10^{-14}$

The dominant term in the common mode gain expression (equation 2.8) is

$$\left.\frac{s\Delta C + \Delta G}{G(G + \Delta G)}\right|_{f=50Hz} = 2\pi \times 10^{3}$$

We note that $s\Delta C$ is over 1000 times larger than ΔG and that their sum is approximately $s\Delta C$. The effect of capacitive mismatch is about 60dB more than that due to resistive mismatch for the same percentage of mismatch. For this reason, capacitive mismatch is the limiting factor for CMRR in biopotential amplifiers. For small values of G, ΔG is not critical to obtain high A_{cm}.

$$\frac{s\Delta C + \Delta G}{G(G + \Delta G)} \approx \frac{s\Delta C}{G(G)}$$

Figure 2-6 is a graph showing the common mode gain of the amplifier in Figure 2-3 under different mismatch scenarios. For this simulation, an ideal opamp was used and 1% of mismatch was introduced between either passive elements to emphasize the importance of capacitive mismatch over resistive mismatch.

It is clearly seen in the figure that the effect of capacitor mismatch on common mode gain is several orders larger than the effect of resistor mismatch. Also, when mismatch is combined in both resistor and capacitor pairs, the overall common mode gain curve follows that of capacitor mismatch within the signal bandwidth.

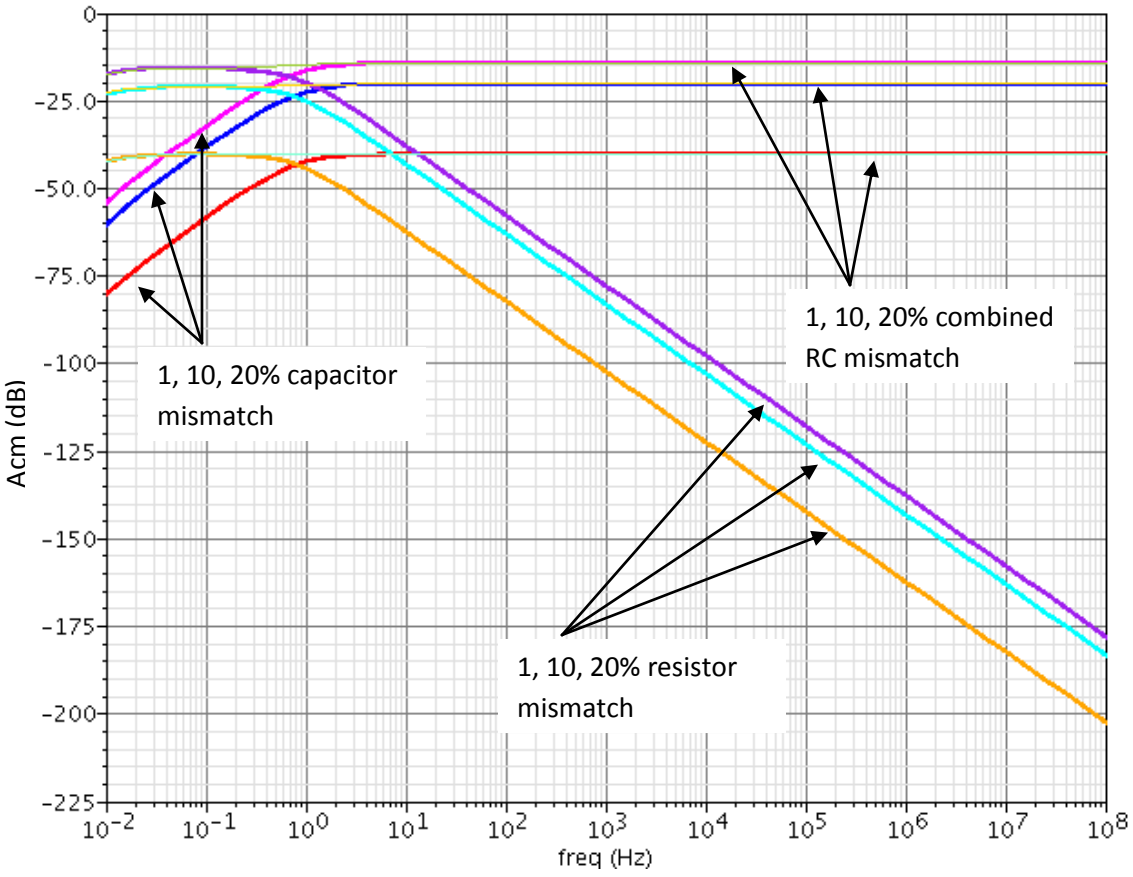

Figure 2-6 Common Mode Gain vs. Frequency of an RC Feedback Amplifier

Since the capacitor mismatch is the limiting factor for CMRR in opamp based biopotential amplifiers, resistor mismatch will be ignored henceforth. To have a better feel for the severity of capacitor mismatch, the common mode response of the

biopotential amplifier of Figure 2-3 is shown for varying percentage of mismatch in Figure 2-5.

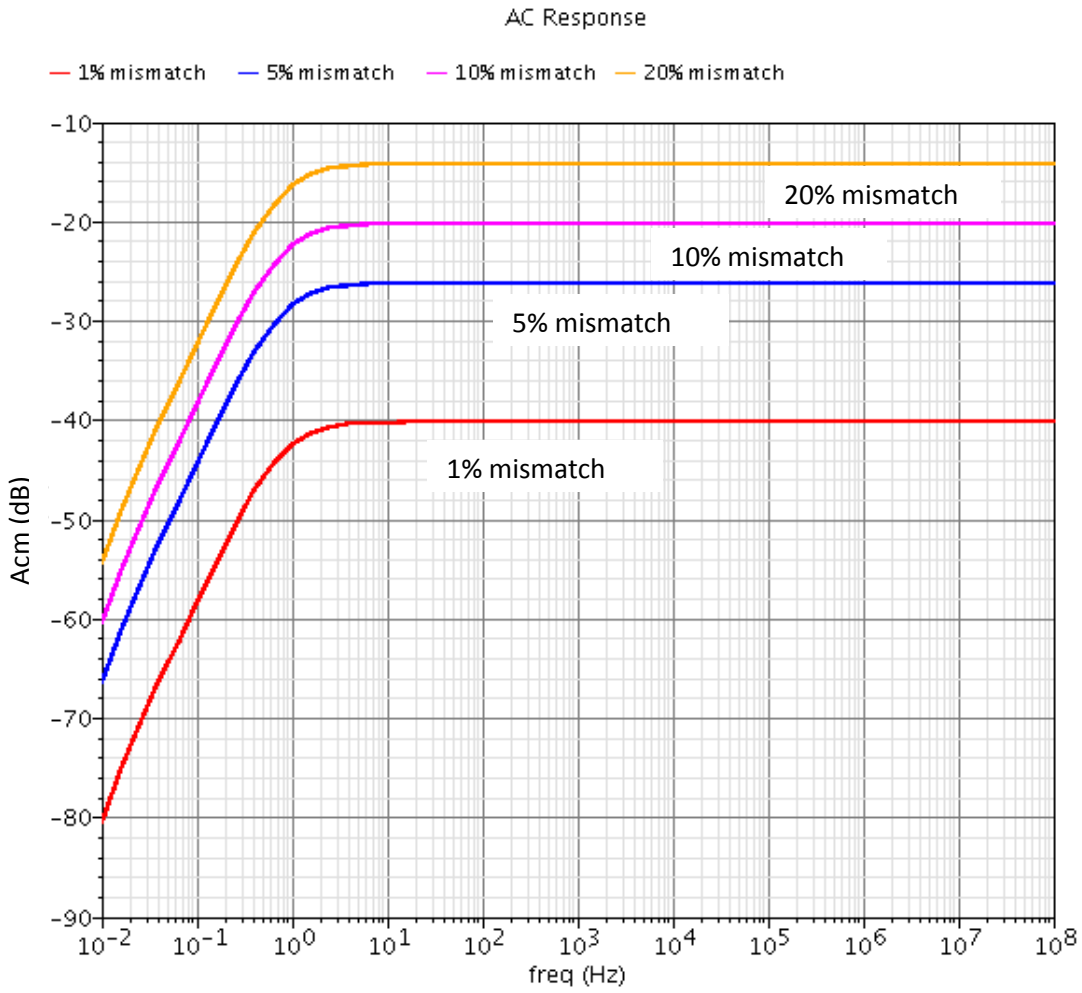

Figure 2-7 Common Mode Gain vs. Frequency for Varying Capacitor Mismatch

Common mode gain (hence CMRR) of the biopotential amplifier degrades with increasing capacitor mismatch. This model assumes ideal components and blocks for the biopotential amplifier. With 1% of capacitor mismatch, common mode gain drops from an infinite amount at mid-band frequencies to about 40dB and it gets worse with

increasing mismatch. This emphasizes how sensitive the CMRR of such biopotential amplifiers is to passive component mismatch.

The other thing to note in Figure 2-5 is the zero at the origin and low frequency pole. The pole zero pair can be explained using equation 2.8. This pole occurs at approximately $1/(C_1R_2)$ and the zero at the origin. However, according to equation 2.8 there should be 1 more pole zero pair.

$$\omega_z \cong \frac{\Delta G}{\Delta C} \quad \text{and} \quad \omega_p \cong \frac{G+\Delta G}{C_1 + C_2 + \Delta C}$$

This pole and zero occur at very low frequency and effectively cancel themselves out thus they do not appear in the frequency response of Figure 2-7. The zero occurs at around 100μHz where as the pole is at less than 10mHz.

Table 2-3 shows common mode gain values of the biopotential amplifier for different percentage mismatch in capacitor. It should be noted that the capacitor mismatch limits the CMRR of the entire biopotential amplifier as has already been explained earlier.

Table 2-3 Common Mode Gain of RC Feedback Biopotential Amplifier at 50Hz

ΔC	**Simulated Ac**	**ΔR**	**Simulated Ac**
0%	-253 dB (infinite)	**0%**	-253 dB (infinite)
1%	-40 dB	**1%**	-76 dB
10%	-20 dB	**10%**	-58 dB
20%	-14 dB	**20%**	-52 dB

The biopotential INA of Figure 2-5 is very simple and easy to design. It is utilizes a single opamp thus making it a low power consuming circuit. The high input impedance

of the opamp makes it suitable for biopotential signal acquisition applications. The problems with this topology are mainly two. First, a very large feedback resistor is required to remove the inherent differential DC offset of biopotential signals that is caused by the difference in half cell potentials of the electrodes used for acquiring the signal. Thus a means is necessary for integrating extra large resistors on chip without consuming excessive silicon area on the die.

The second issue with this topology is the poor CMRR and very high sensitivity of common mode gain to mismatch of capacitors. The first problem of implementing large resistors on chip has been overcome in some previous works and in this thesis, a solution is proposed to the second problem of poor CMRR.

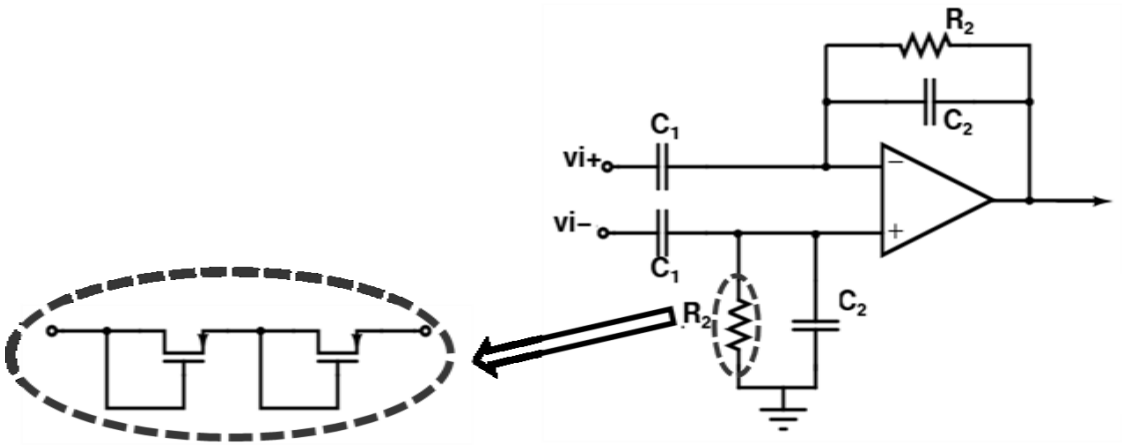

Figure 2-8 Biopotential Amplifier with MOS-Bipolar Pseudo Resistor Element

D. Previously Published Works on Biopotential Amplifiers

1. A Low Power Low Noise CMOS Amplifier for Neural Recording Applications

The work in [1] is based on the simple RC feedback circuit shown of Figure 2-5. It is classified under the opamp based biopotential amplifiers. It has a bandpass filter with the lower cutoff frequency in the sub hertz range. To achieve such a small cutoff frequency,

a very large RC time constant has to be implemented and this achieved using a bipolar-MOS pseudo resistor circuit.

The pseudo resistor is essentially two diode connected PMOS transistors that are connected in series shown in Figure 2-8. With negative vgs values, the circuit functions as a normal diode connected PMOS transistor. However with positive values of vgs, its functions as a diode connect pnp transistor [12]. With small voltage values across the diode series connection, a very high incremental resistance (in the gig ohm range) is achieved and hence a large time constant. This circuit can be designed to be low noise and low power consuming but it still suffers from poor CMRR due to capacitor mismatch. The reported CMRR for this work is 86dB but this is an average across the signal bandwidth. The good CMRR at very low frequencies improves the average CMRR.

2. Versatile Integrated Circuit for Acquisition of Biopotentials [9]

The instrumentation amplifier shown in Figure 2-9 is an extension of the work done in [1]. It has two amplification stages the first being similar to circuit of Figure 1-6 except that it is made fully differential. The second stage is equivalent to the input stage of the classic three – opamp instrumentation amplifier. This is done to give fully differential outputs and to split overall INA gain between the two stages.

Again with this topology, a MOS-bipolar pseudo resistor element is used to achieve the large time constant necessary for removing the differential DC offset of the electrodes. As with the topology in [1], this circuit still suffers from poor CMRR due to capacitor mismatch. The reported value for CMRR at mid-band frequencies is 70 dB.

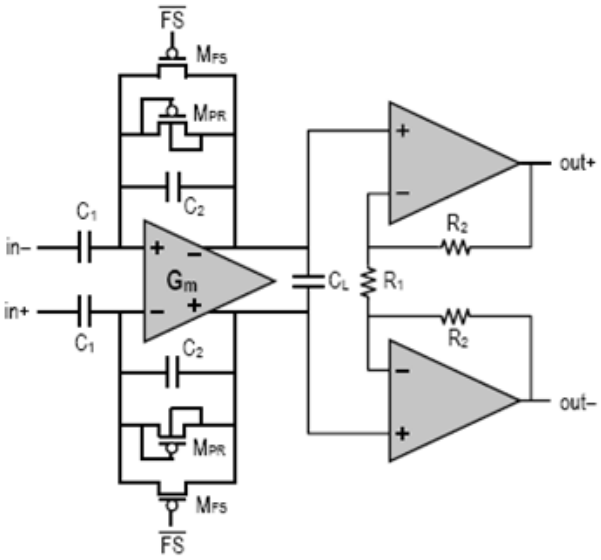

Figure 2-9 Two Stage INA with Fully Differential Outputs

3. A 60nw, 60nv Readout Front End for Portable Biopotential Signal Acquisition

The core instrumentation amplifier in this work [3] is of the Current Balancing/ Current Feedback type. It includes three choppers that are used to reduce the flicker noise of the INA. It is referred to as an AC Coupled Chopped Instrumentation Amplifier (ACCIA) in the published work. A block diagram of the ACCIA is shown in Figure 2-10.

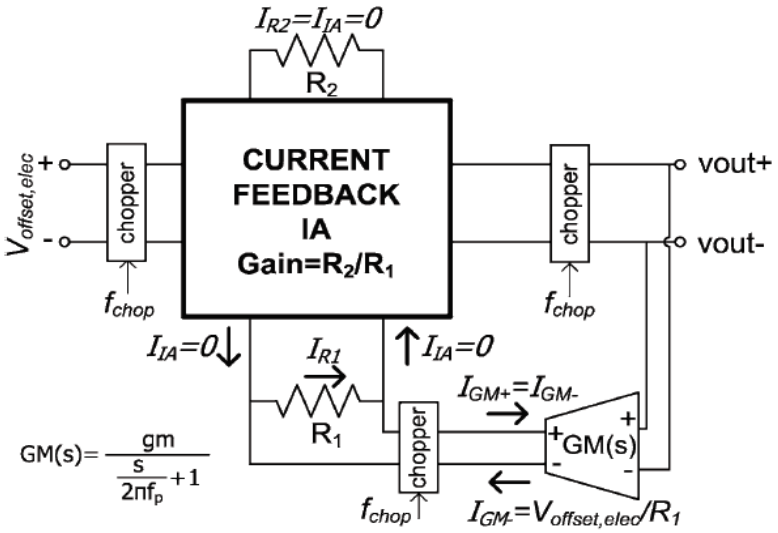

Figure 2-10 Concept of ACCIA [3]

The mid-band gain of the INA is defined as the ratio of R2 to R1. The biopotential signal is first up-converted from its based frequency to some intermediate frequency where the actual amplification is performed. Afterwards it is down-converted to obtain the output signal. There is a further up-conversion and filtering of the output signal in the feedback stage. This is done to extract the DC offset of the output biopotential signal and subtract it that of the input and in the process cancel out the offset so it does not appear in the final amplified output. The ACCIA is implemented as shown in Figure 2-11. The core current balancing amplifier is based on [2] published by Steyaert.

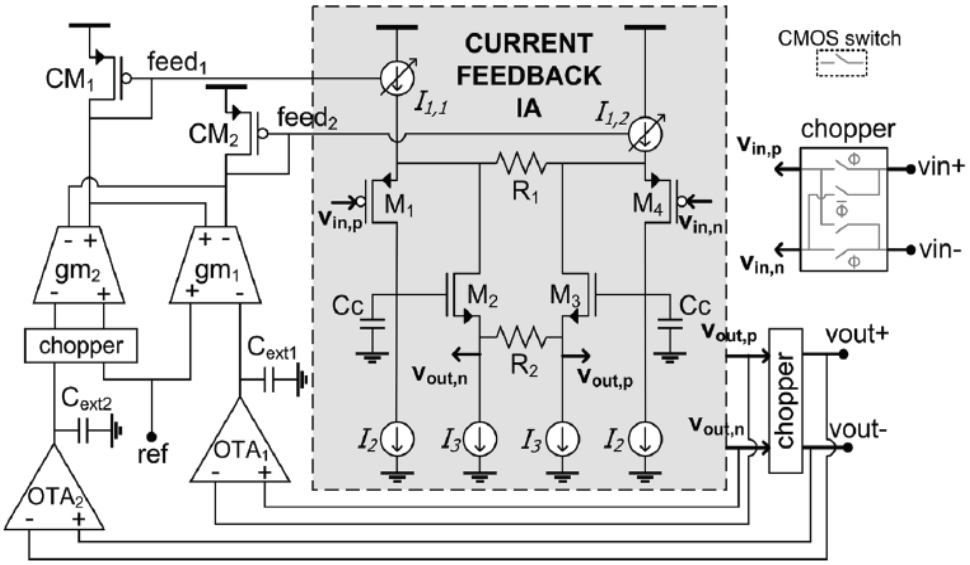

Figure 2-11 Implementation of ACCIA

As with all current balancing topologies, this INA has good CMRR performance however its complexity is high. The reported CMRR is 110dB. Also, the gain of the INA is not well defined. Under ideal circumstances the gain if defined by the resistive ratio of R2 to R1. However, simulations of this circuit show that the gain can deviate by over 50% from the desired value and thus makes the design unpredictable and unreliable as well.

In the next section, an instrumentation amplifier is proposed based on the simple topology of [1] with a way of fixing the poor CMRR normally associated with such INAs.

3. PROPOSED INSTRUMENTATION AMPLIFIERS

In the previous sections, the issue of poor CMRR due to mismatch of passive components in opamp based INAs was thoroughly analyzed. Currently, techniques used to improve matching are usually done after fabrication and these include laser trimming of the passive elements such as resistors and some other calibration techniques. Any other technique for improving the matching between the passive elements should also lead to significant improvement in CMRR of the INA.

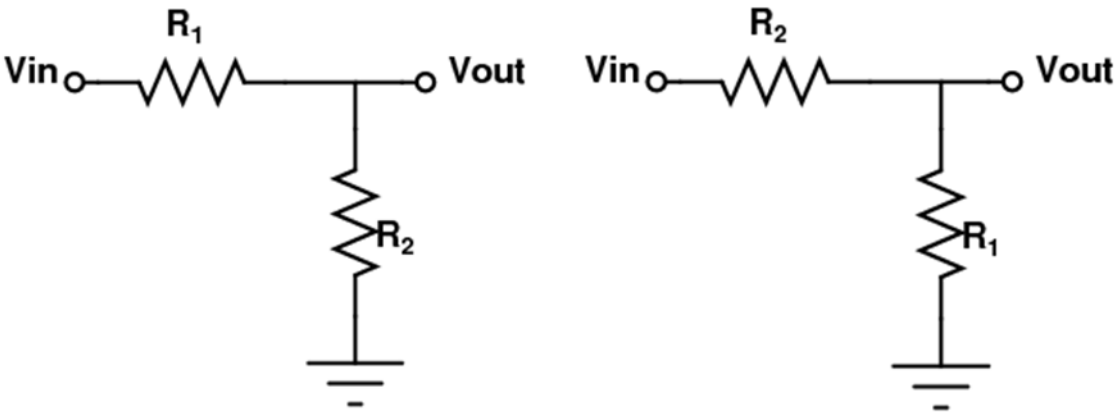

Figure 3-1 Simple Voltage Divider Using Resistors

A. Dynamic Element Matching

Dynamic Element Matching (DEM) is a well known technique used in data converter systems to improve DNL (Differential Non-Linearity) and INL (Integrated Non-Linearity) specifications [13],[14]. It does this by averaging the mismatch of the resistors in the DAC/ ADC string. Different algorithms exist for implementing DEM schemes ranging from very simple to quite complex in data converters.

The effect of DEM can be demonstrated using the resistor divider circuit of Figure 3-1. Suppose we want to generate an output voltage Vout, that is exactly half of the input voltage Vin, then we need the resistors R_1 and R_2 to be equal in value with no zero mismatch. However, if R_1 varies slightly from R_2, then the actual output voltage is defined as in equation 3.1.

$$V_{out} = \left(\frac{R_2}{R_1 + R_2}\right) V_{in} \quad \text{.....(3.1)}$$

To ensure that Vout is exactly half of Vin, the resistors R_1 and R_2 could be interchanged several times per period (hypothetically) and instead of seeing the effect of individual resistors, the output voltage would be defined by an effective resistance as shown in equations 3.2 and 3.3. This is essentially the aim of any dynamic element matching scheme; To average the value of different passive elements over a period to reduce the effect of mismatch on circuit performance.

$$R_{eff} = \frac{R_1 + R_2}{2} \quad \text{... ... ... (3.2)}$$

$$V_{out} = \left(\frac{R_{eff}}{2R_{eff}}\right) V_{in} \quad \text{.....(3.3)}$$

B. Concept of Proposed INAs

The idea for the proposed instrumentation amplifier for biopotential signal acquisition is to first design a simple low power opamp based INA and implement simple DEM scheme to average out the effect of mismatch in the passive elements so as to improve CMRR. We start from the basic biopotential acquiring INA in Figure 2-3 and make it

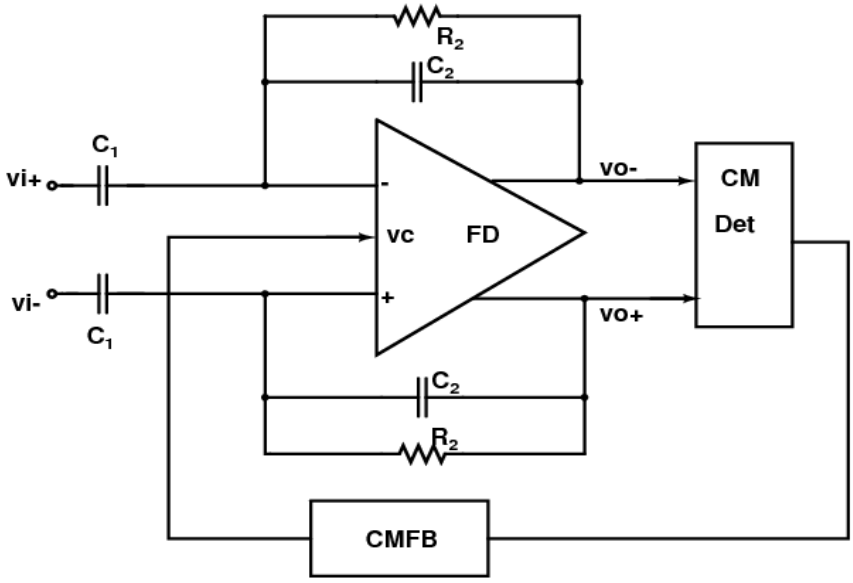

Figure 3-2 Fully Differential Version of INA

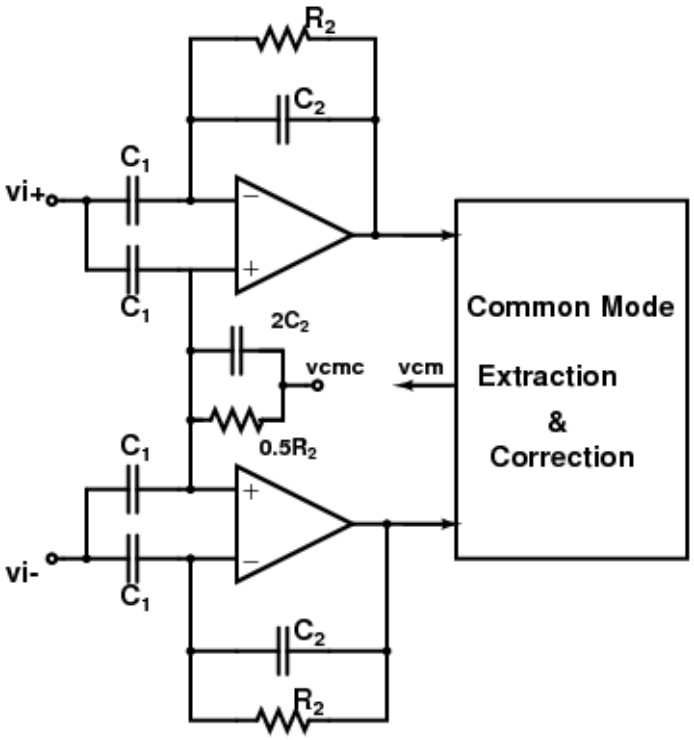

Figure 3-3 Fully Balanced Fully Symmetric Version of INA

fully differential. To make it fully differential, we can just use a single fully differential opamp or use two single ended opamps in a fully balanced fully symmetric topology. These two methods are shown in Figures 3-2 and 3-3.

It has already been shown in previous sections that mismatch between the resistors is less critical than mismatch of capacitors. As such CMRR can be greatly improved if mismatch between the corresponding capacitors pairs is eliminated as much as possible.

The common mode gain can be expressed as a function of capacitor mismatch as shown below. This is obtained from equation 2.8 and assuming perfect matching between the resistors.

$$A_{cm}(s) = \frac{V_o}{V_{icm}} = \frac{s\Delta C}{G(G)} \cdot \frac{sC_1}{\left(1 + s\frac{C_1 + C_2 + \Delta C}{G}\right)} \cdot \frac{1}{1 + s\,{}^{C_2}\!/_{G}} \quad \ldots\ldots\ldots\ldots\ldots (3.4)$$

An inverse Laplace transform can be performed on this expression and this gives the time domain response of the biopotential amplifier to common mode signals.

$$A_{cm}(t) = \frac{1}{2\pi j} \lim_{T\to\infty} \int_{-T}^{T} e^{st} A_{cm}(s)\,ds \quad \ldots\ldots\ldots\ldots\ldots\ldots\ldots\ldots\ldots (3.5)$$

In other words, the time domain equivalent of the common mode gain is obtained by integrating the $A_{cm}(s)$ over the period of the biopotential signal being amplified. It is important to realize this since it implies that any mismatch in capacitors is also being integrated over a period to form the time domain signal.

The capacitor mismatch is defined as

$$\Delta C = C_1 - C_2$$

$$-\Delta C = C_2 - C_1$$

If the polarity (algebraic sign) of ΔC can be reversed several times in a period, then according the equation 3.5, the time domain signal can be rid of any common mode output since the integral of $A_{cm}(s)$ would approach zero.

1. Conceptual Block Diagram

Thus the next step logically is to figure out a way to reverse the polarity of the capacitor mismatch several times within the period of the biopotential signal being processed.

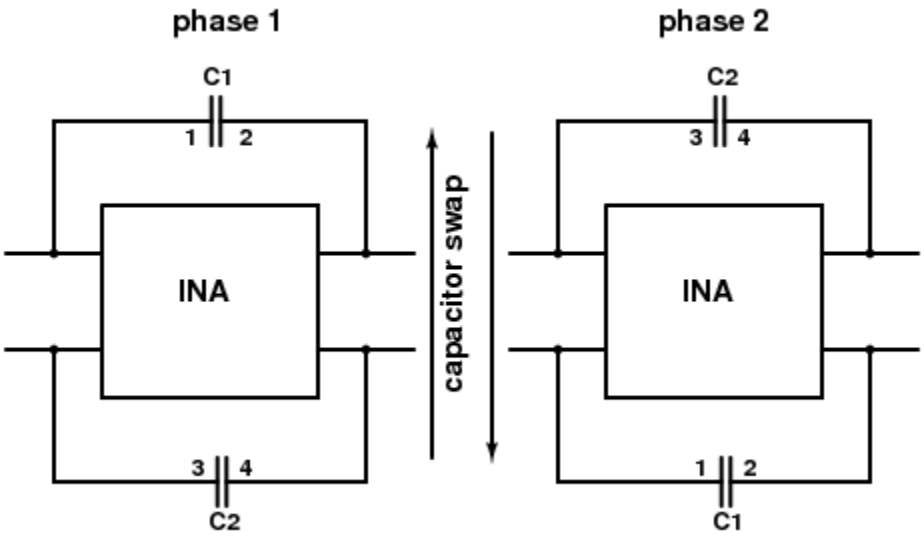

Figure 3-4 Swapping of Capacitors to Reverse Polarity of Mismatch

One conceptual way to achieve this is to physically swap the capacitors several times per period. In phase 1 of Figure 3-4, C1 is connected to the upper feedback path while C2 is connected to the bottom feedback path. In the second phase, C1 and C2 are physically interchanged such that C2 is now connected to the upper feedback path. The effect of doing this several times per period is the same as was seen in equation 3.2 and the effective capacitance is the average value of capacitors C1 and C2.

This physical swapping of capacitors is not feasible on chip but the same effect can be emulated by using switches together with the capacitors pairs that have to be matched. This is explained with the diagram in Figure 3-5.

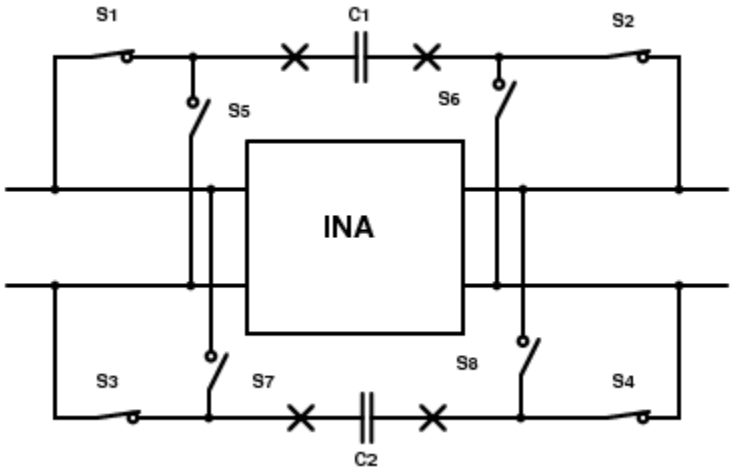

(a) phase 1

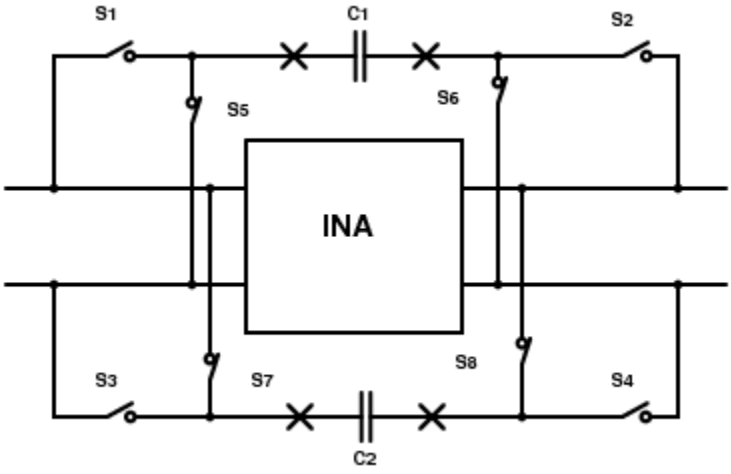

(b) phase 2

Figure 3-5 Emulating the Effect of Swapping Capacitors using ON/ OFF Switches

Eight switches are required to emulate the effect of physically swapping two capacitors. The capacitors are connected to the switches which are in turn connected to the appropriate nodes of the INA. In phase one of Figure 3-5a, C1 is connected to the upper feedback network of the INA through switches S1 and S2 whereas C2 is connected to the bottom feedback network through switches S3 and S4. Switches S5 to S8 are entirely OFF in this phase. In the second phase shown in Figure 3-5b, switches S1 to S4 switch OFF while S5 to S8 switch ON. Thus C2 connected to the upper feedback network in this phase whereas C1 is connected to the bottom feedback section.

This is essentially the same as dynamically matching capacitors C_1 and C_2 and the effective value of the feedback capacitance over a time period is the average of C1 and C2.

This technique is applied to the fully differential and fully balanced fully symmetric circuits shown in Figures 3-2 and 3-3. Two sets of capacitors have to be matched in each circuit and thus a total of 16 switches are required to emulate the effect of physically swapping the capacitors pairs several times within the period of the biopotential signal.

C. Dynamically Matched RC Feedback Fully Differential INA

The first of the proposed instrumentation amplifiers is obtained by applying capacitor swapping technique to the fully differential RC feedback amplifier of Figure 3-2. The capacitors that have to be matched are the two input capacitors pairs, $C_{1,}$ and the two feedback capacitor pairs, C_2. Eight switches are used for dynamically matching each pair of capacitors resulting in a total of sixteen switches.

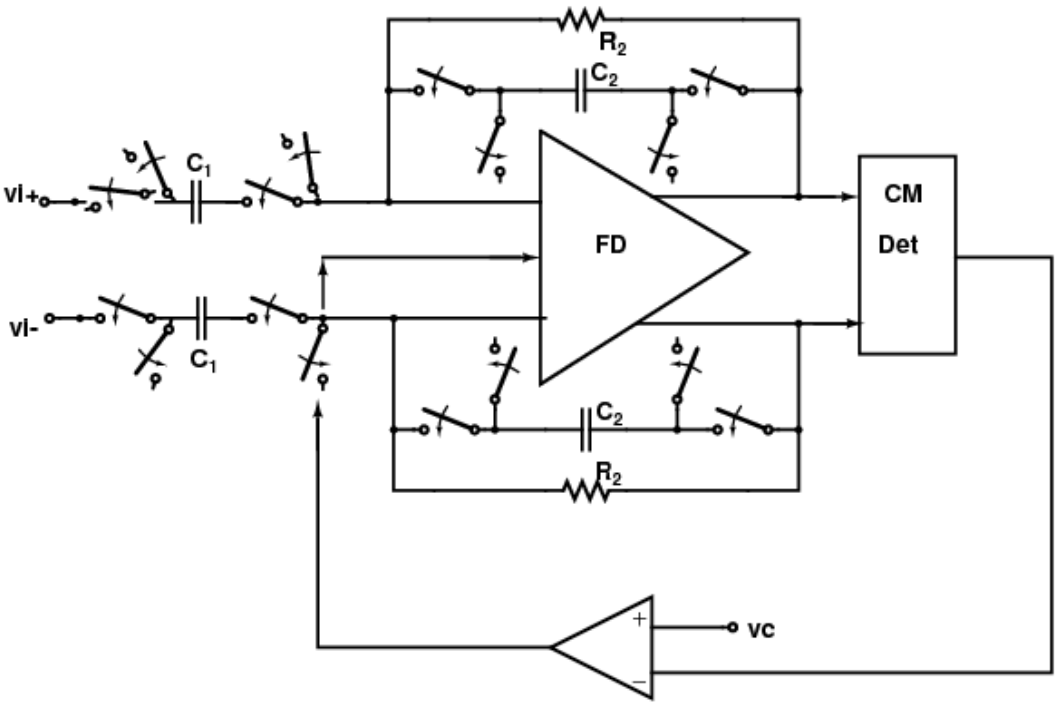

Figure 3-6 Fully Differential Version of Dynamically Matched INA

A fully differential operational amplifier is used as FD shown in Figure 3-6, thus extra circuitry is required for common mode detection and correction. This is also shown in Figure 3-6.

D. Dynamically Matched RC Feedback FBFS INA

The fully balanced fully symmetric (FBFS) version has four sets of capacitors to be matched however only two pairs need to be dynamically matched. A different technique can be used to compensate for the effect of capacitor mismatch between any pair of capacitors that lie on the circuit's axis of symmetry. This will be explained further in the next sections.

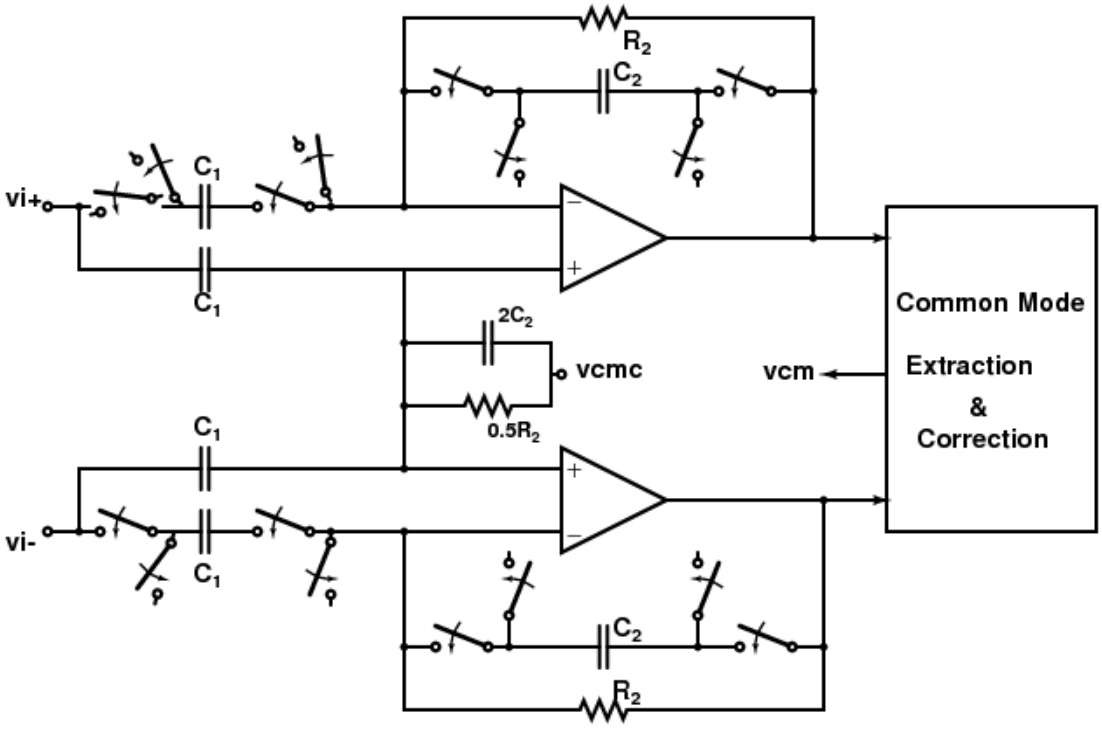

Figure 3-7 Dynamically Matched FBFS INA

The dynamically matched fully balanced fully symmetric INA of Figure 3-7 employs two single ended opamps to generate differential outputs. Since single ended amplifiers are used, the common mode feedback circuit is not always necessary for this topology. There are however some benefits to be obtained by using CMFB.

1. Test of Balanced Conditions in Fully Balanced Fully Symmetric Systems

For any fully balanced fully symmetric topology, the property in equation 3.6 below holds true. The equation parameters are shown in Figure 3-8.

$$\frac{V_{o1}(s) + V_{o2}(s)}{2V_{iR}} = 1 \quad \text{.....(3.6)}$$

That is if a signal is injected into the node at the axis of symmetry of the amplifier, the resulting common mode output signal should be exactly equal to the injected voltage. This criterion can be used to test for symmetry and balanced conditions for any fully balanced fully symmetric topology.

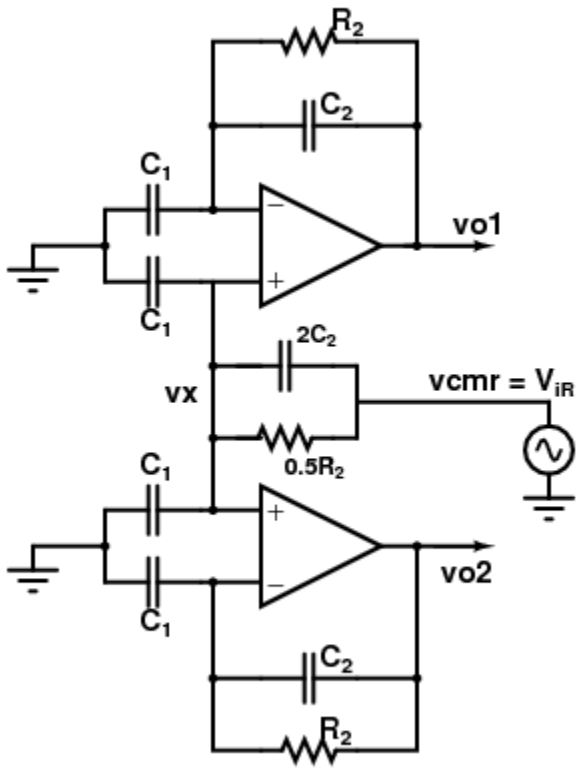

Figure 3-8 Test for FBFS Amplifier

A direct consequence of this property is that if the common mode output signal of the amplifier is corrected and fed back to this common output node, symmetry and balanced conditions can be forced on the amplifier. This is the same as implementing a common mode feedback scheme on the fully balanced fully symmetric topology. This is what shown in proposed INA of Figure 3-7. There are four pairs of capacitors that have to be matched however only two pairs are dynamically matched where as the other two pairs that are connected to the axis of symmetry of the circuit have their mismatch corrected by correcting the output common mode signal and injecting it into the common mode output node using a common mode feedback scheme (CMFB).

E. System Level Design

In this section, the design of the proposed INAs at the system level is discussed. First we decide the targeted specifications of our INAs after which we determine the values of the capacitors required to meet those specification. The gain, gain bandwidth product and noise requirements of the opamps used for the INA are also determined systematically. The system level design of both the fully differential and fully balanced fully symmetric dynamically matched INAs is similar.

For this work, the biopotential amplifier is designed for acquiring EKG signals. EKG signals have the amplitude and frequency characteristics shown in Table 3-1.

Table 3-1 Amplitude and Frequency Characteristics of EKG

Amplitude	**Frequency Range**
0.1mV – 5mV	0.5Hz – 150Hz

To acquire the EKG signal the instrumentation amplifier is designed with the target specifications in Table 3-2.

Table 3-2 Target Specifications of EKG Signal Amplifier

Parameter	**Specification**
CMRR	> 100 dB
Input Referred Noise	2-3μV rms
Input Impedance	> 5MHz
Bandwidth	0.5 – 150 Hz
Gain	40 dB

1. Determining Capacitor and Resistor Values

To determine the capacitor sizes to meet the target specifications, we first design the proposed instrumentation amplifiers assuming there was no dynamic element matching.

With this assumption, the differential mode transfer function for the INAs is as shown in equation 3.7.

$$\frac{V_{out}}{V_{in}} = \frac{sC_1R_2}{1 + sC_2R_2} \quad \text{.....(3.7)}$$

The mid-band gain and high pass filter corner frequency are defined as below.

$$\text{mid-band gain (G)} = \frac{C_1}{C_2} \quad \text{.....(3.8)}$$

$$\text{high pass corner freq } (f_H) = \frac{1}{2\pi R_2 C_2} \quad \text{.....(3.9)}$$

Capacitor C_1 is selected to be large based on the available area on the die and C_2 is obtained from equation 3.8. For this design the following values are used.

$$\text{Let } C_1 = 20\text{pF}, G = 4\ 0\text{dB} = 100$$

$$C_2 = \frac{C_1}{G} = 200\text{fF}$$

$$\text{Thus } C_1 = 20\text{pF and } C_2 = 200\text{fF}$$

From the specification table and using equation 3.9

$$f_H = 0.5\text{Hz and } R > \frac{1}{2\pi f_H C_2} > 1.6 \text{ Tohm}$$

With the MOS-bipolar pseudo resistor element, very large incremental resistances in the tera-ohm range can be realized on chip [12]. Table 3-3 shows final component values.

Table 3-3 Final Component Values for Proposed INAs

Component	**Value**
C1	20 pF
C2	200 fF
R2	> 1.6 Tohm

2. Determining Opamp Specifications

We seek to determine the following specifications for the opamps used in the INAs.

- Open Loop Gain
- Gain Bandwidth Product
- Input Referred Noise

2.1 Gain

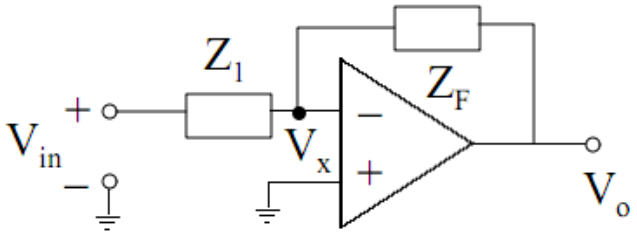

Figure 3-9 Inverting Opamp Configuration

The open loop gain of the opamp defines the accuracy of the closed loop gain. For the inverting opamp shown in Figure 3-9, the actual closed loop gain is defined as in shown below in equation 3.10 if the finite open loop gain of the opamp is taking into account.

$$\frac{V_o}{V_{in}} = \frac{\frac{Z_f}{Z_1}}{1+\frac{1}{A}\left(1+\frac{Z_f}{Z_1}\right)} \dots\dots\dots\dots\dots\dots\dots\dots\dots\dots\dots (3.10)$$

This expression applies not only to inverting amplifier configurations but to others as well. A more general expression is given in equation 3.11 where A_c is the closed loop gain.

$$A_c(\text{actual}) = \frac{A_c(\text{desired})}{1+\frac{1}{A}\left(1+\frac{Z_f}{Z_1}\right)} \dots\dots\dots\dots\dots\dots\dots\dots\dots\dots (3.11)$$

$$\text{accuracy} = \frac{1}{1+\frac{1}{A}\left(1+\frac{Z_f}{Z_1}\right)}$$

$$accuracy \cong 1-\frac{1}{A}\left(1+\frac{Z_f}{Z_1}\right) \dots\dots\dots\dots\dots\dots\dots\dots\dots\dots (3.12)$$

For about 95% closed loop gain accuracy with 40dB gain, equation 3.12 requires the open loop gain of the opamp to be greater than 1919 (65 dB).

2.2 Gain Bandwidth Product

The instrumentation amplifier is designed to have a bandpass filter characteristic with the high pass filter cutoff frequency defined by the feedback resistor and capacitor and the low pass filter cutoff defined by the gain bandwidth product of the opamp.

$$GBW = A_0\omega_{3dB} = A_cBW$$

where A_0=opamp open loop gain A_c=INA closed loop gain BW=Signal Bandwidth

For EKG, the signal bandwidth is about 150 to 200 Hz, therefore

$$GBW \geq 200 \times 1000Hz = 200KHz$$

Another way to determine GBW of the opamp is to use the accuracy requirement. Assuming a non-ideal opamp with a pole at the origin, then the closed loop accuracy of the amplifier is defined as

$$accuracy \cong 1 - \frac{s}{GBW}\left(1 + \frac{Z_f}{Z_1}\right)$$

If the opamp has a pole at the origin, then the GB of the opamp has to be greater than 200kHz for 95% accuracy and greater than 1MHz for 99% accuracy.

The minimum GBW for the opamp is 200 kHz however the opamp will be designed to have a larger GBW as an extra design precaution.

2.3 INA Input Referred Noise

The input referred noise for the instrumentation amplifier shown in Figure 3-10 is derived assuming ideal capacitors with no parasitic resistance. Under these constraints, the dominant noise contributors are the resistors and the opamp. First we consider the effect of opamp noise on the overall INA.

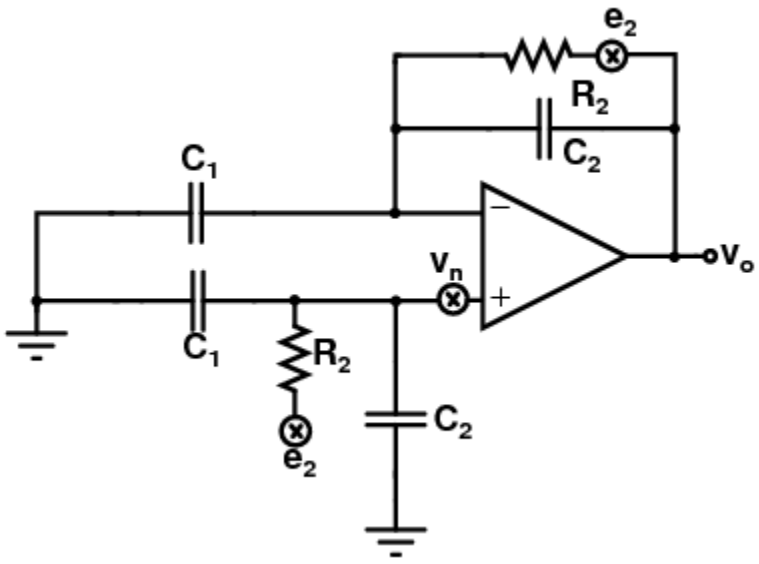

Figure 3-10 INA for Noise Analysis

Let the input referred noise of the opamp be $v^2_{n(in)}$ and $v^2_{n(out)}$ be the output noise.

$$v^2_{n(out)_{INA}} = v^2_{n(in)} \left(1+\frac{Z_f}{Z_1}\right)^2 = v^2_{n(in)} \left(1+\frac{sC_1R_2}{1+sC_2R_2}\right)^2$$

$$v^2_{n(out)\_INA} = v^2_{n(in)} \left(\frac{1+s[(C_1+C_2)]R_2}{1+sC_2R_2}\right)^2$$

The input referred noise of the INA is obtained as shown below in equation 3.13.

$$\text{gain}_{(\text{INA})} = \frac{sC_1R_2}{1+sC_2R_2}$$

$$v^2_{n(in)_{INA}} = \frac{v^2_{n(out)_{INA}}}{(gain)^2} = v^2_{n(in)} \left[\frac{1+sR_2(C_1+C_2)}{sC_1R_2}\right]^2 \quad \text{.....(3.13)}$$

$$v^2_{n(in)_{INA}} \approx v^2_{n(in)} \left[\frac{1+sC_1R_2}{sC_1R_2}\right]^2 \approx 1 \text{ (at mid-band frequencies)} \text{.....(3.14)}$$

Next we consider the noise due to the grounded and feedback resistors, R2. Let the noise voltage of the resistors be e_2.

$$E^2_{2out} = e_2^2 + \frac{e_2^2}{[1+sR_2(C_1+C_2)]^2}\left[1+\frac{sC_1R_2}{1+sC_2R_2}\right]^2$$

$$= e_2^2 + \frac{e_2^2}{[1+sR_2(C_1+C_2)]^2}\left[\frac{1+s(C_1+C_2)R_2}{1+sC_2R_2}\right]^2$$

$$\text{Output noise due to Resistors, } R_2 = E^2_{2out} = e_2^2 + \left[\frac{e_2}{1+sC_2R_2}\right]^2$$

$$\text{Input Referred Noise due to , } R_2 = E^2_{2in} = \frac{e_2^2 + \left[\frac{e_2}{1+sC_2R_2}\right]^2}{gain_{INA}}$$

At mid-band frequencies, the input referred noise of the INA is entirely equal to the noise of the opamp. The noise of both resistors is attenuated by the INA gain. The grounded resistor has further attenuation due to the pole in its transfer function.

Table 3-4 Final Opamp Target Specifications

Specification	**Target**
Gain	65 dB
Gain Bandwidth Product	1.0 MHz
Input Referred Noise	3 μV rms

F. Transistor Level Design

In this section, the design of the opamp, MOS – Bipolar pseudo resistor, non – overlapping clock generator and switches are detailed at the transistor level. We begin with the opamp design for the dynamically matched fully differential INA. The specifications are shown in Table 3-4. The INAs are designed using 0.5µm ON Semi process parameters.

1. Fully Differential Opamp Design

The topology used for this design is an adaptation of the work in [15] to make it fully differential and used with a dual supply rails. This topology is chosen mainly because it is a single stage low power, low noise yet high CMRR opamp. It is basically a telescopic amplifier with PMOS input transistors and a cascode current mirror as the tail current. The transistor level schematic diagram is shown in Figure 3-11.

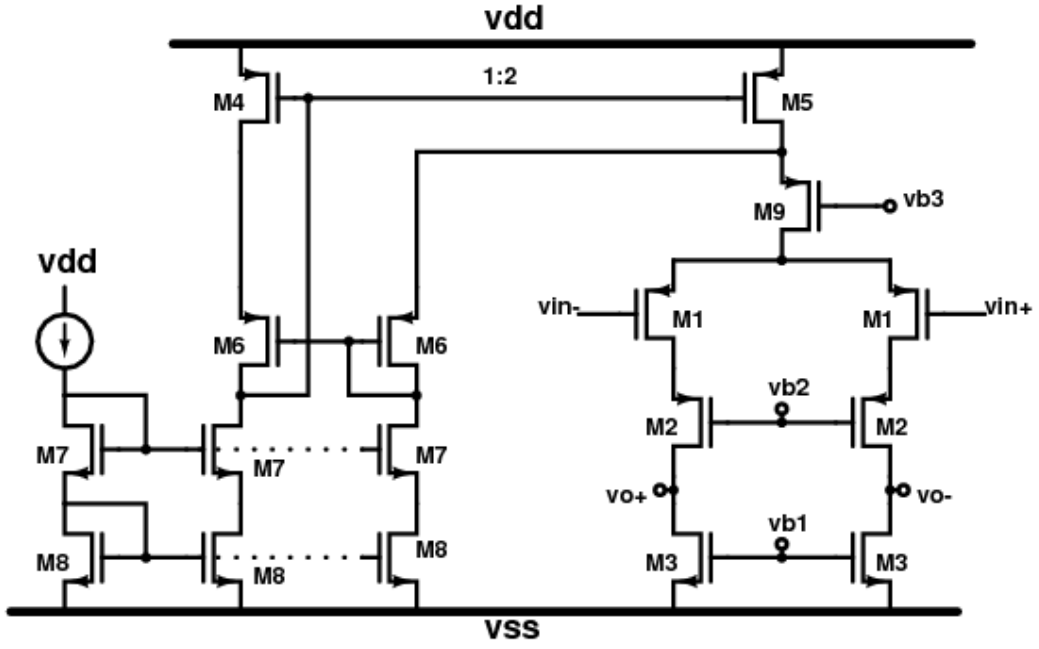

Figure 3-11 Transistor Level Schematic Diagram of Fully Differential Opamp

The differential gain and common mode gain for the amplifier are shown below.

$$A_{dm} = g_{m1}R_{out}, \text{ where } R_{out}=r_{o3}//(g_{m2}r_{02}r_{o1})$$

$$A_{cm} = \frac{g_{m1}Y_s}{2g_{m1}+Y_s}, \quad \text{where } Y_s=\frac{1}{g_{m9}r_{o9}r_{o5}}$$

1.1 Design Procedure

1. First we establish the design equations for this opamp. The gain and GBW of the opamp are defined as shown below.

$$A_o = g_m R_{out} = 65dB$$

$$GBW=\frac{g_m}{C_L}=1MHz \quad C_L\approx 10pF, \ \therefore g_m=10\mu A/V$$

2. The load capacitance is assumed to be 10pF since this is the typically value of the input capacitance of the probes of an oscilloscope. We design the gm of the input transistors, M1 to have 10μS of transconductance.

$$gm=\sqrt{\mu Cox\frac{W}{L}I_{BIAS}} \qquad \text{.....(3.15)}$$

3. Using equation 3.15 and typical values of PMOS μCox for the 0.5μm process ($35\mu A/V^2$) and using a bias current of 1μA, W/L of M1 is determined to be 5.

$$W/L\ (M1) = 5$$

4. Transistors M4 – M9 are sized to properly bias the opamp and to mirror the correct currents. The M5:M4 current mirror is sized 2:1 whereas all other mirrors are sized 1:1.

5. Transistors M2 and M3 are sized to meet the gain and noise requirements of the opamp. An iterative procedure is used which is explained in the next section.

$$\text{gain}=g_m R_{out}=65\text{dB}\approx 2000$$

$$g_m=\frac{10\mu A}{V} \text{ therefore } R_{out} > 200 \text{ Mohm}$$

$$R_{out}=r_{o3} // (g_{m2} r_{o2} r_{o1}) \approx g_{m2} r_{o2} r_{o1}$$

(r_{o3} is very large due to large L used to reduce flicker noise)

$$\text{Let } g_{m2}=100\mu \text{ and } r_{o2}=r_{o1}$$

$$\text{then } r_{o1} = r_{o2} = \sqrt{\frac{R_{out}}{g_{m2}}} = 1.4 \text{ Mohm}$$

L is determined using the lambda of the transistors. $\Lambda = 0.1$ to 0.5.

$$L=\frac{1}{\lambda r_o} \cong 1.4\mu\text{m to } 7\mu\text{m}$$

W is determined from the basic transistor current equation

$$W=\frac{2IL}{\mu C_{ox}(V_{DSAT})^2} \text{ , } I=1\mu, V_{DSAT}=0.2 \text{ and } \mu C_{ox(PMOS)}=40\mu$$

$$W \approx 2\mu\text{m to } 8\mu\text{m}$$

The bode magnitude and frequency plots of the opamp are shown in Figure 3-12.

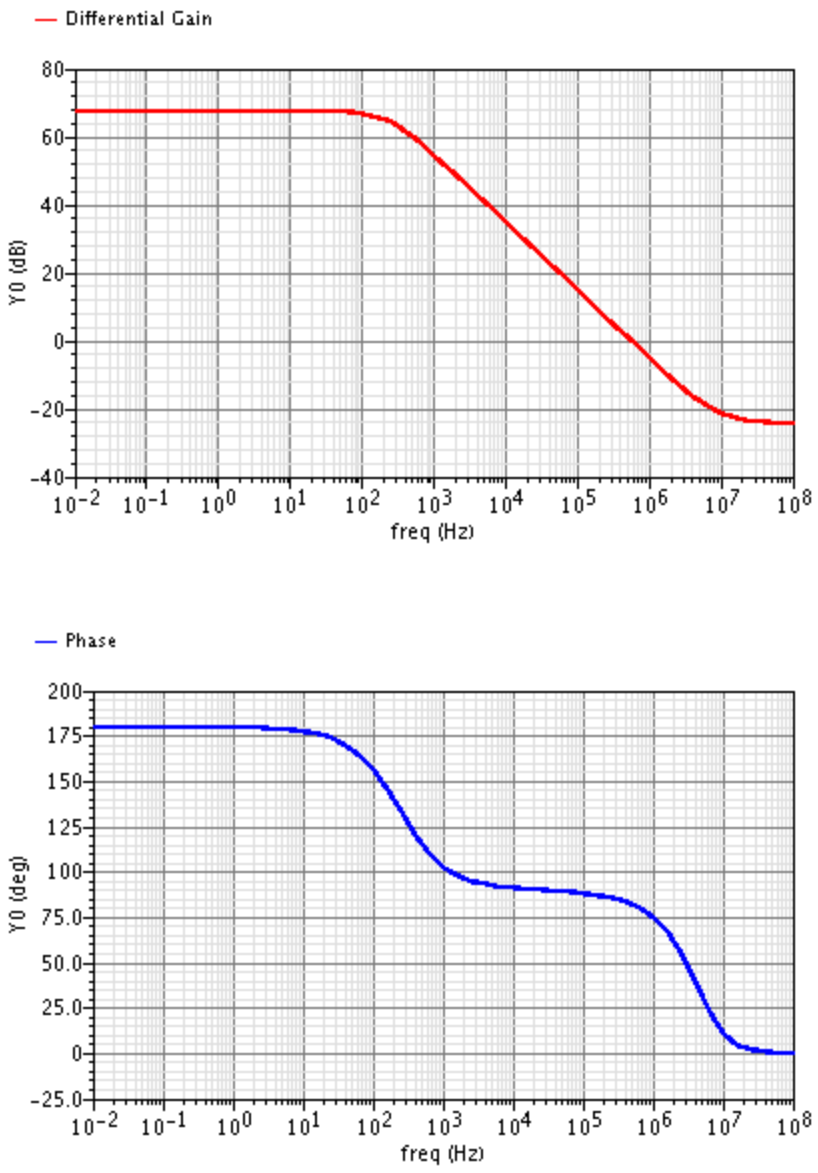

Figure 3-12 Differential Frequency Response of Designed Opamp

1.2 Noise Consideration

The dominant noise contributors are the input PMOS transistors, M1 and the NMOS load transistors, M3.

$$I_N^2 = 2I_{N(M1)}^2 + 2I_{N(M3)}^2$$

Thermal Noise Contribution

$$I_{N(thermal)}^2 = 8KT[g_{m1} + g_{m3}]$$

Flicker Noise Contribution

$$I_{N(flicker)}^2 = \frac{K_f}{\mu C_{ox} WLf}$$

Referring total noise contribution to the opamp inputs gives

$$V_{N(\text{input referred})}^2 = \frac{1}{g_{m1}^2}\left[8KT[g_{m1} + g_{m3}] + \frac{K_f}{\mu C_{ox} WL_{(M1)} f} + \frac{K_f}{\mu C_{ox} WL_{(M3)} f}\right] \ldots\ldots (3.16)$$

K_f is the flicker noise co-efficient of the transistors. There are different ways of reducing the noise input referred noise of INAs. Chopping is one technique commonly used and typically removes low frequency noise and offset of the amplifier [7],[8],[10]. Another technique is to carefully size the transistors to reduce the low frequency flicker noise and the white noise as well. As is shown in equation 3.16, flicker noise is inversely proportional the area of the transistor's conducting channel. Moderate to large WL products can be used to reduce flicker noise of the INA. This is the noise reduction option that is used for this INA design.

From equation 3.16, gm1 has to be increased while the transistor M1 and M3 sizes have to also be made large. To meet the gain specification as well, we increase the length of M3 iteratively while checking if the noise specification is met. The effect of increasing the size of transistor M3 on noise performance is shown in Figure 3-13.

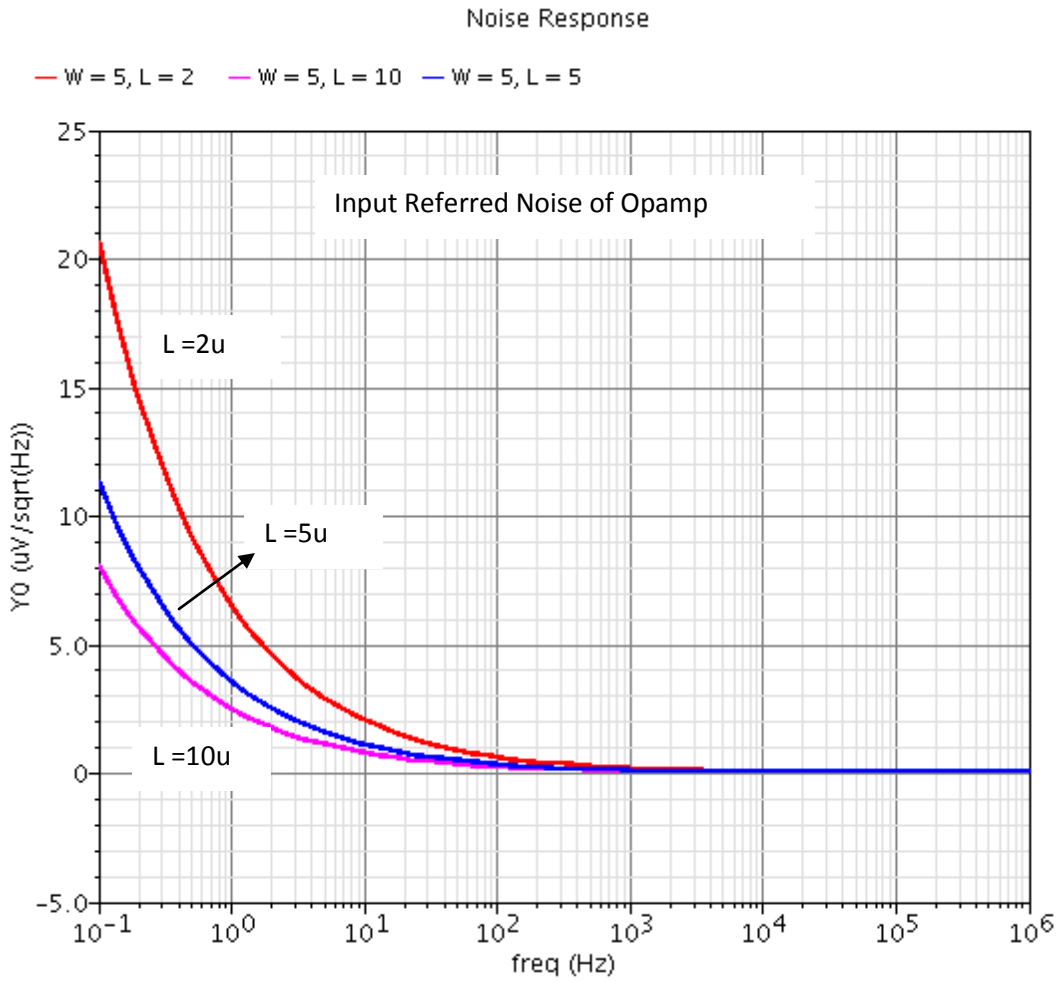

Figure 3-13 Effect of Transistor M3 Sizing on Input Referred Noise

For the plots in Figure 3-13, the width of M3 was kept constant while the length was varied. The input referred noise is plotted for each combination of transistor width and length. It is clearly seen that to reduce the flicker noise, large transistor sizes must be used. Whereas the transistor width could also be increased reduce the flicker noise, it is more practical to increase the length for layout purposes. Also increasing the length gives the additional benefit of increasing the gain of the opamp at the same time.

Transistor sizes for the fully differential INA are shown in Table 3-5.

Table 3-5 Transistor Sizes for Fully Differential Opamp

Transistor	**Aspect Ratio**	**Fingers**
M1	5/1	16
M2	5/2	4
M3	5/10	1
M4	5/2	4
M5	5/2	8
M6	5/2	4
M7	5/2	4
M8	5/2	4
M9	5/2	4
Ibias	1 μA	

2. Common Mode Feedback Circuit

The common mode feedback circuit used with the fully differential amplifier is shown in Figure 3-14. The outputs of the fully differential opamp vary between ± 500mV extremes and the CMFB loop is designed to have large enough gain and be stable about this common mode range of inputs. Transistor sizes used for the CMFB circuit are shown in Table 3-6.

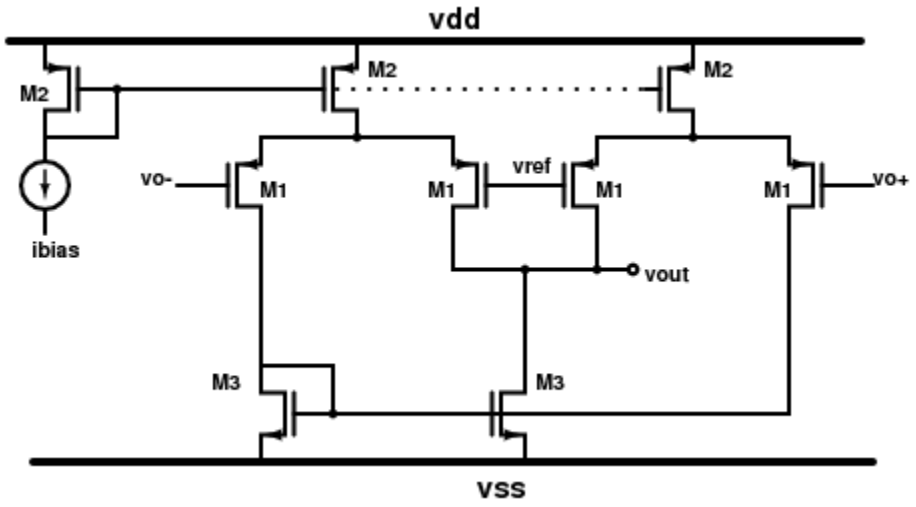

Figure 3-14 Common Mode Feedback Circuit for Opamp

$$A_v = \frac{v_{out}}{v_{o+} - v_{o-}} = g_{m1}(r_{o3} // r_{o1})$$

Table 3-6 Transistor Sizes for CMFB Circuit

Transistor	**Aspect Ratio**	**Fingers**
M1	5/3	4
M2	5/2	4
M3	5/10	1

3. Single Ended Opamps for Fully Balanced Fully Symmetric INA

The opamps used in the FBFS INA are of the topology in [15]. Thus, the design is exactly the same as with the design of the fully differential version. The transistor level schematic is shown in Figure 3-15 with transistor dimensions in Table 3-7.

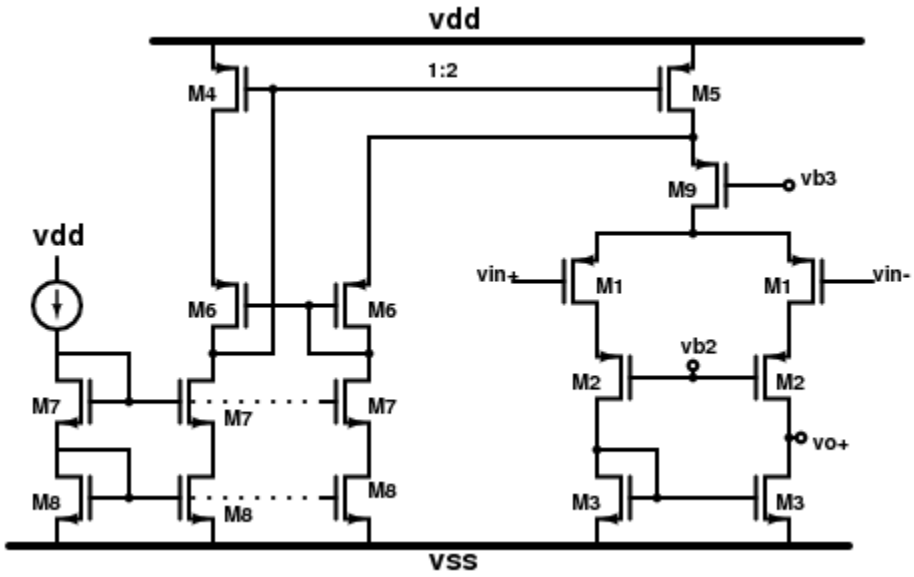

Figure 3-15 Transistor Level Schematic Diagram of Single Ended Opamp

Table 3-7 Transistor Sizes for Single Ended Opamps in FBFS INA

Transistor	Aspect Ratio	Fingers	Transistor	Aspect Ratio	Fingers
M1	5/1	16	**M6**	5/2	4
M2	5/2	4	**M7**	5/2	4
M3	5/10	1	**M8**	5/2	4
M4	5/2	4	**M9**	5/2	4
M5	5/2	8			

4. Design of Non-overlapping Clock Generator

Two opposite phased clocks are required for implementing the proposed INAs. It is essential that at any point in time, no two switches connected to the same node be ON at the same time. Using two individual but opposite phased clocks does not guarantee that this condition can be met. As such, a two-phase non-overlapping clock generator is required for this function. A typical digital CMOS implementation is shown in Figure 3-16. It takes a single clock signal as its input and outputs two opposite phased non-overlapping clocks. There is a dead zone between the two output clock signals in every period where neither clock output is high. Figures 3-17 and 3-18 show the operation.

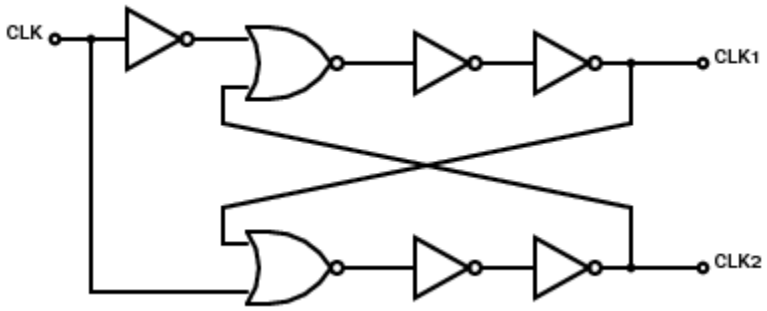

Figure 3-16 Two-phase Non-overlapping Clock Generator

The digital gates were designed using static CMOS to minimize the static power consumption of the INAs. Sizing of the gates is shown in Table 3-8.

Table 3-8 Aspect Ratios of Static CMOS Gates

Gate	**NMOS**	**PMOS**
NOR	4/2	16/2
NOT	4/2	8/2

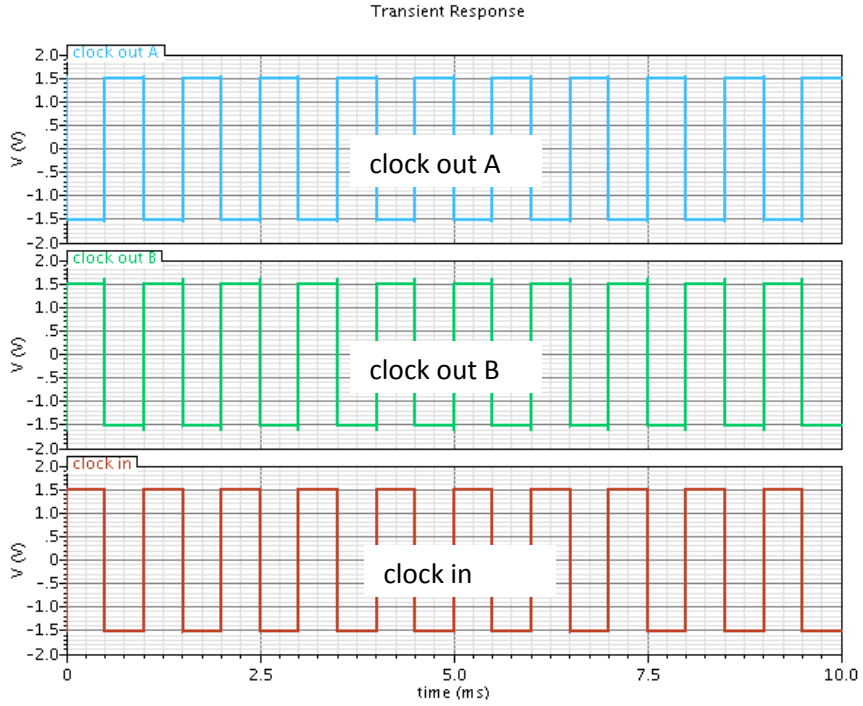

Figure 3-17 Outputs of Non-overlapping Clock Generator

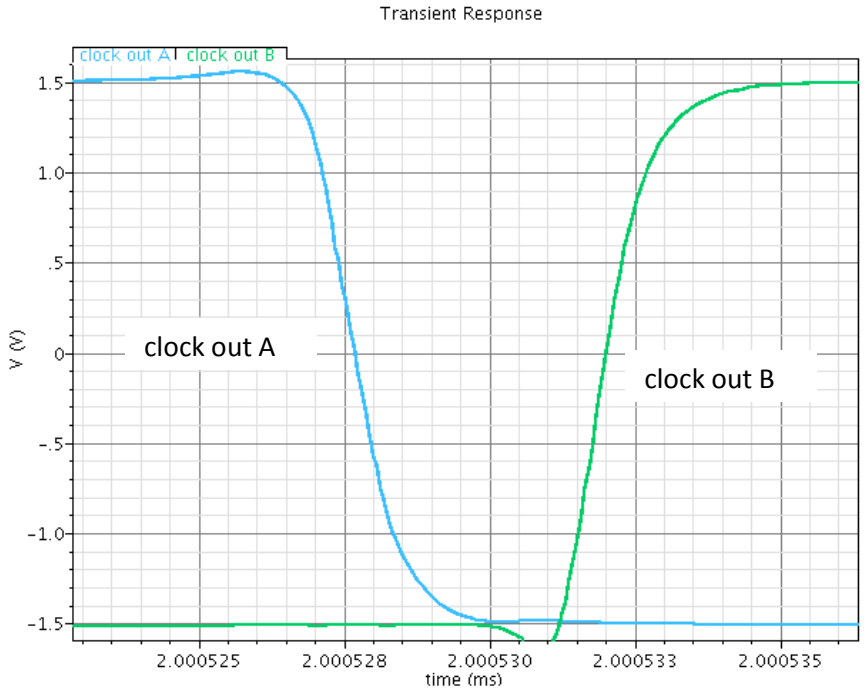

Figure 3-18 Snapshot of Non-Overlapping Region of Clocks

5. MOS – Bipolar Pseudo Resistor Element

The large RC time constant required for the very low cutoff high pass corner frequency is generated using the MOS-Bipolar pseudo resistor element as in [1]. Two diode connected PMOS transistors are used to implement this eliminating the need for biasing the transistors. Figure 3-19 shows the incremental resistance of the element.

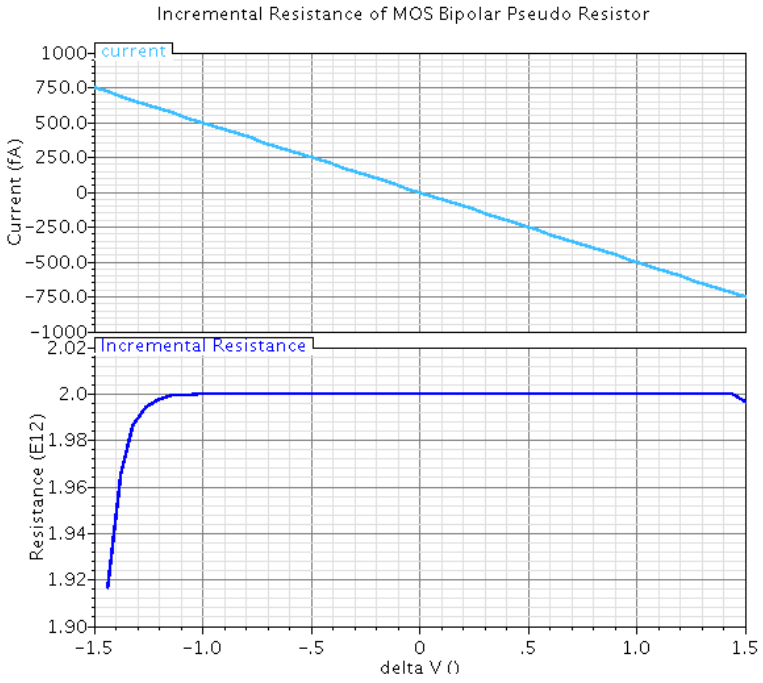

Figure 3-19 Incremental Resistance of Pseudo-resistor Element

It is seen from the figure that incremental resistance in the teraohm range can be attained using this technique. For the result shown, the transistor dimensions in Table 3-9 were used.

Design Procedure

1. Start with minimum L and choose a suitable W convenience for the transistor and obtain plots of incremental resistance vs. voltage as shown in Figure 3-19.

2. Increase L as necessary if incremental resistance is less than desired.

Table 3-9 Aspect Ratios of Pseudo Resistor Element

PMOS Width	PMOS Length
3μm	2μm

6. Switch Implementation

There are three main options to consider for switch implementation; NMOS switches, PMOS switches or transmission gates. Of these three, NMOS switches were used for this design mainly because they have the smallest switch ON resistance while using small transistor dimensions to reduce any parasitic capacitances. Large gate to source or gate to drain capacitances introduces clock feed-through when a clock is applied to the gate of the switch.

$$I=\frac{\mu C_{ox} W}{L}\left[V_{DS}(V_{GS}- V_T) - \frac{V_{DS}^2}{2}\right]$$

$$\text{switch ON conductance}=\frac{dI}{dV_{DS}}=\mu C_{ox}\left(\frac{W}{L}\right)(V_{GS}- V_T)$$

The V_{GS} is the clock signal and is 1.5 volts. V_T for the process used is 0.7 volts. With these parameters, the switch width and length below in Table 3-10 are used.

Table 3-10 Sizing of Switches

NMOS Width	NMOS Length
1.0μm	0.6μm

4. LAYOUT STRATEGY AND SIMULATION RESULTS

A. Layout

A good layout is always necessary to optimize the performance of any integrated circuit. This INA includes switches, capacitors, opamps, and non-overlapping clock circuitry. As much as possible, the layout is made symmetrical so that variations across the silicon die and wafer impact the symmetrical parts of the circuit in the same way. Figures 4-1 to 4-4 show the layouts of the two proposed INAs.

1. Layout of Dynamically Matched Fully Differential INA

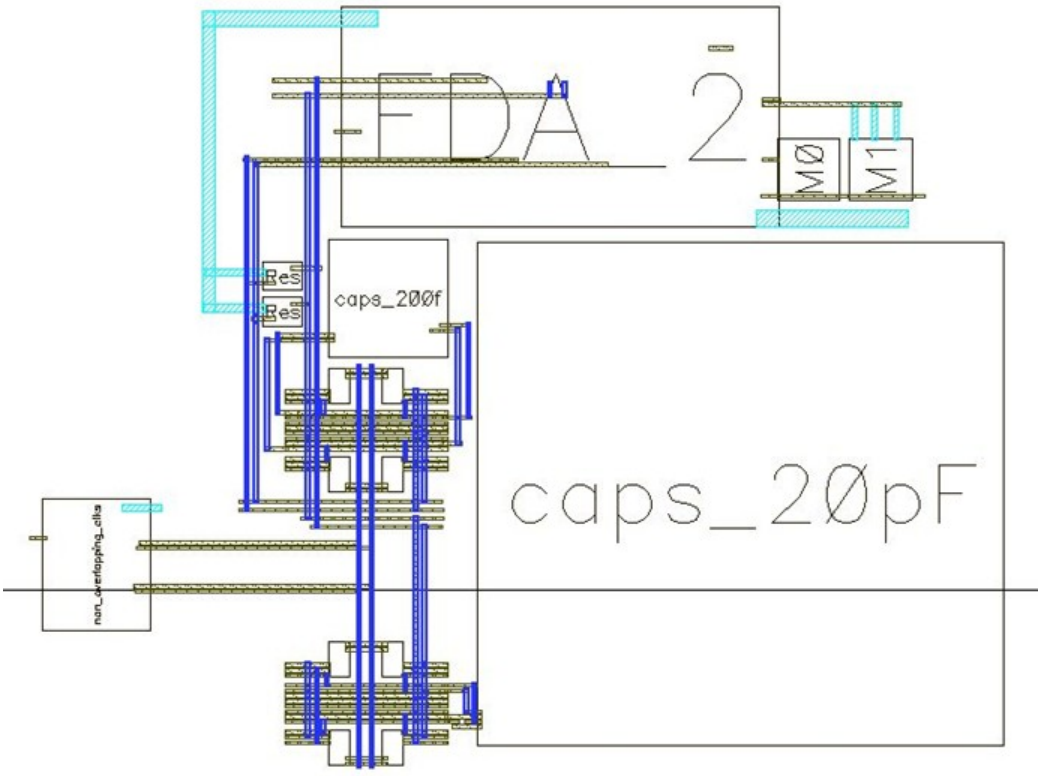

Figure 4-1 Top Level Layout of Fully Differential INA

2. Top Level Layout of Dynamically Matched Fully Balanced Fully Symmetric INA

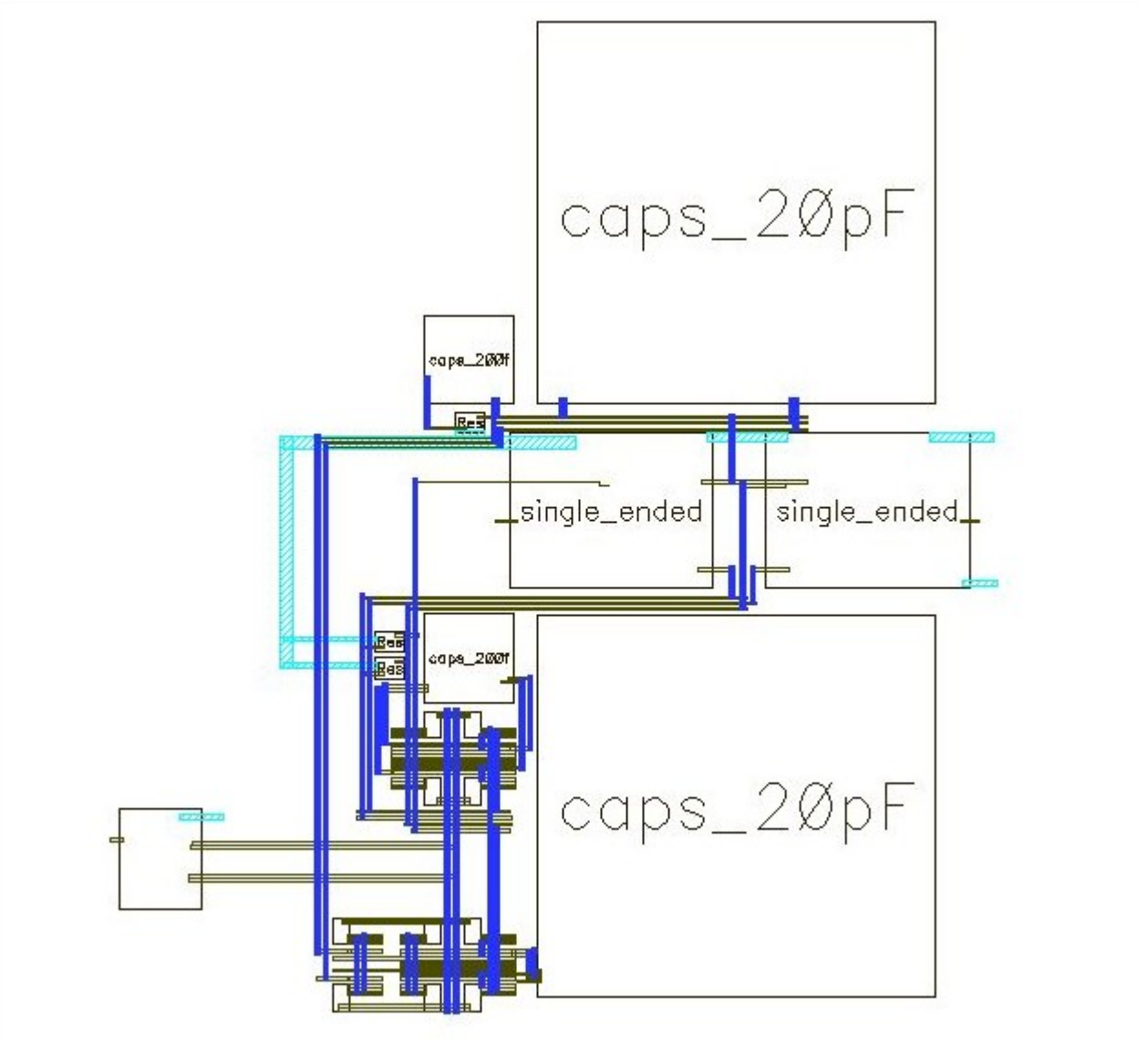

Figure 4-2 Top Level Layout of Dynamically Matched Fully Balanced Fully Symmetric INA

3. Top Level Layout of Proposed INAs in Silicon Die

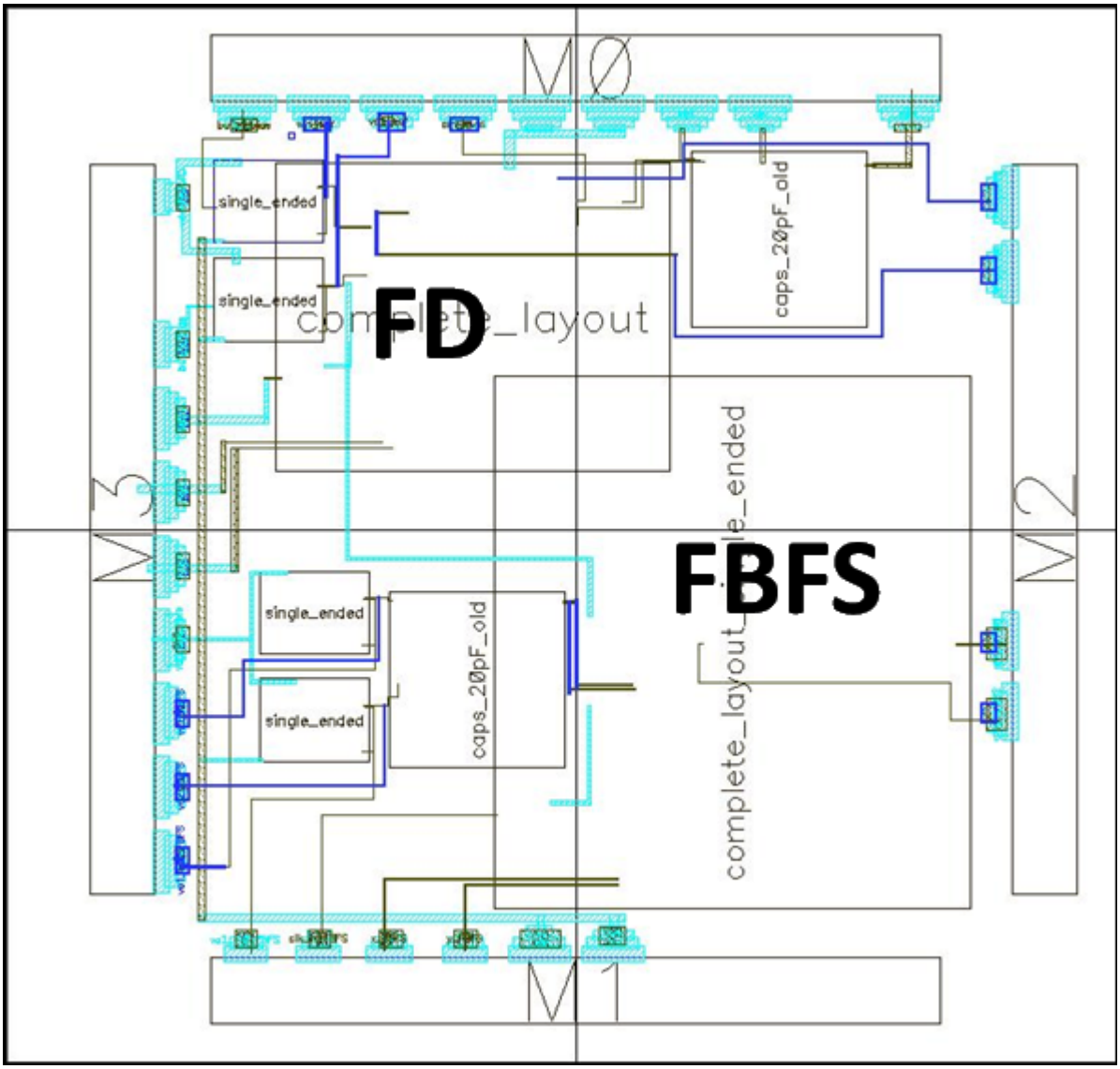

Figure 4-3 Top Level Floor Plan of Proposed INAs in Die

4. Complete Layout of INAs in Silicon Die

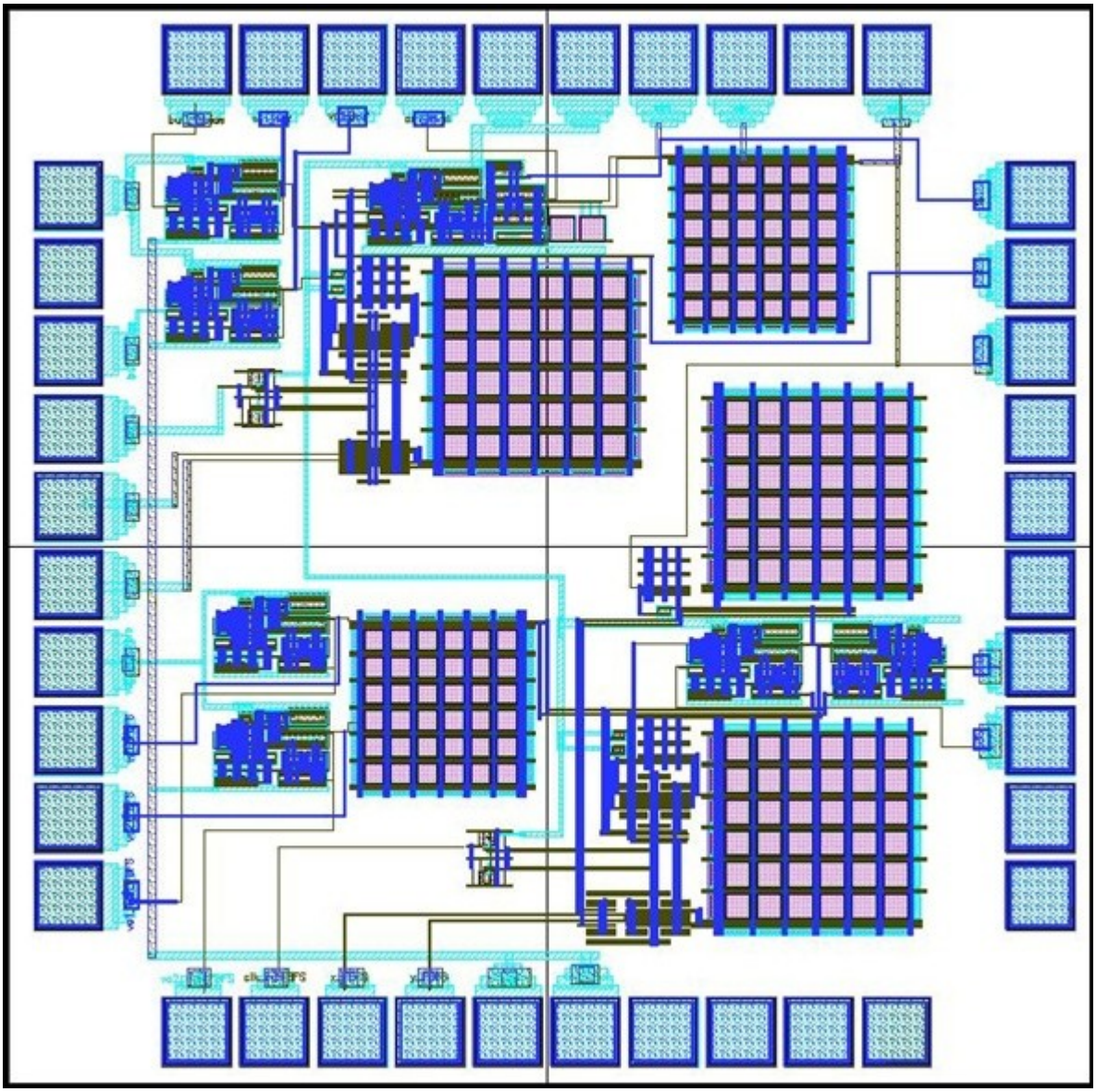

Figure 4-4 Complete Layout of INAs in Silicon Die

B. Results – Dynamically Matched Fully Differential INA

1. Time Domain Signal

Figure 4-5 shows a transient simulation of the dynamically matched fully differential INA. A 50Hz, 2mV pk-pk input signal is applied and the voltages at the outputs of the feedback capacitors and the output of the overall INA are shown. The effect of emulating the swapping of capacitors is seen in the switching of the voltage measured at the capacitor terminals. It is also seen that the INA output is a perfect reconstruction of the feedback capacitor terminal voltages.

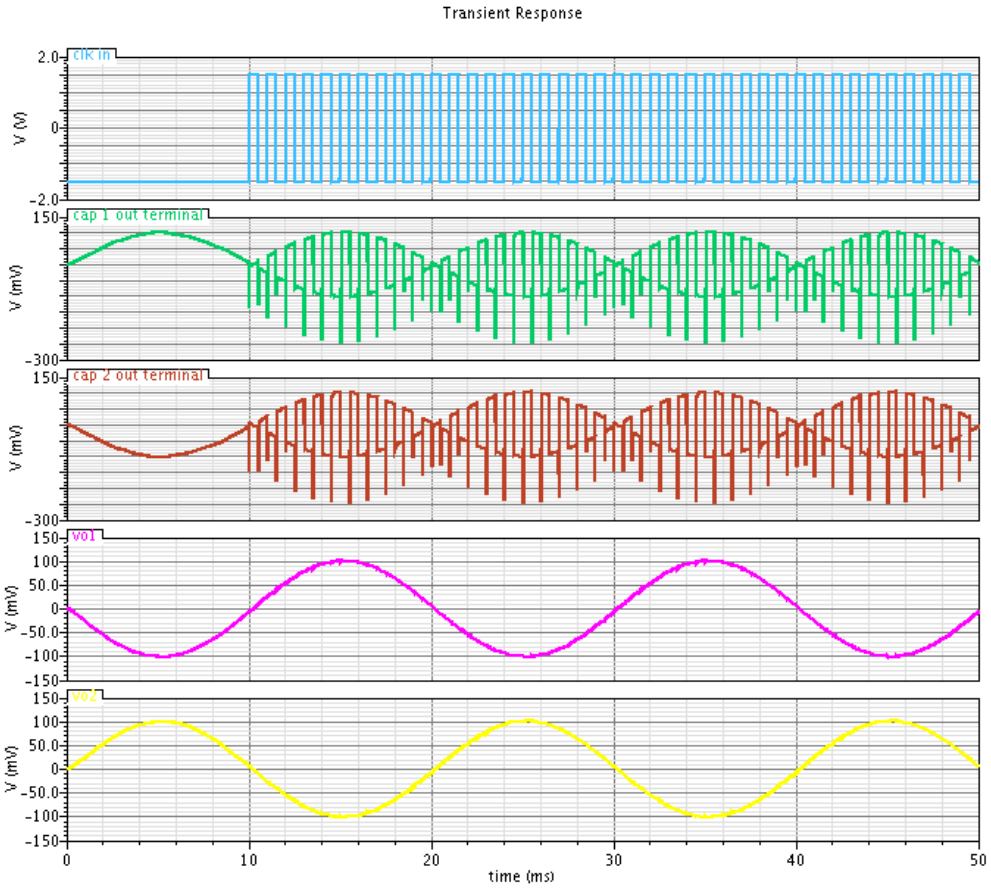

Figure 4-5 Transient Simulation of Fully Differential INA

2. Differential Mode Frequency Response

Next we check the differential mode frequency response of the INA. The bode magnitude and phase plots for the INA are shown in Figure 4-6 when a differential signal is applied to it. We observe a high pass corner frequency of 0.4 Hz and a low pass corner frequency of 1.0 kHz as was designed for. The mid-band gain is also 40 dB as defined by the capacitor ratio.

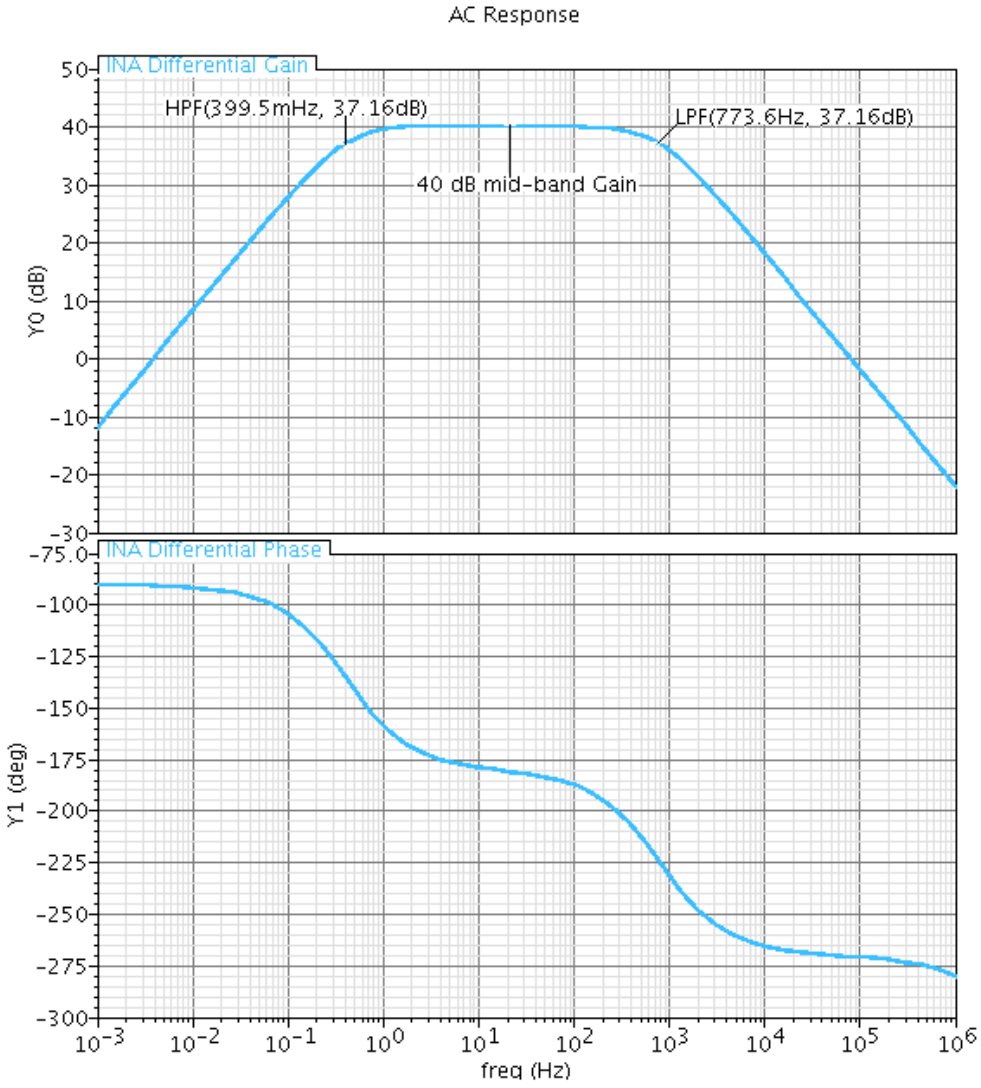

Figure 4-6 Differential Mode Frequency Response of Dynamically Matched Fully Differential INA

3. Common Mode Frequency Response and Common Mode Rejection Ratio

The common mode gain of the dynamically matched fully differential INA is shown in Figure 4-7. Notice that the common mode gain of the INA is better than -150 dB for all frequencies of interest (dc to 100 Hz) and this implies a CMRR better than `90 dB within the signal bandwidth. The INA was designed targeting EKG acquisition and the typical signal bandwidth is about 150 Hz.

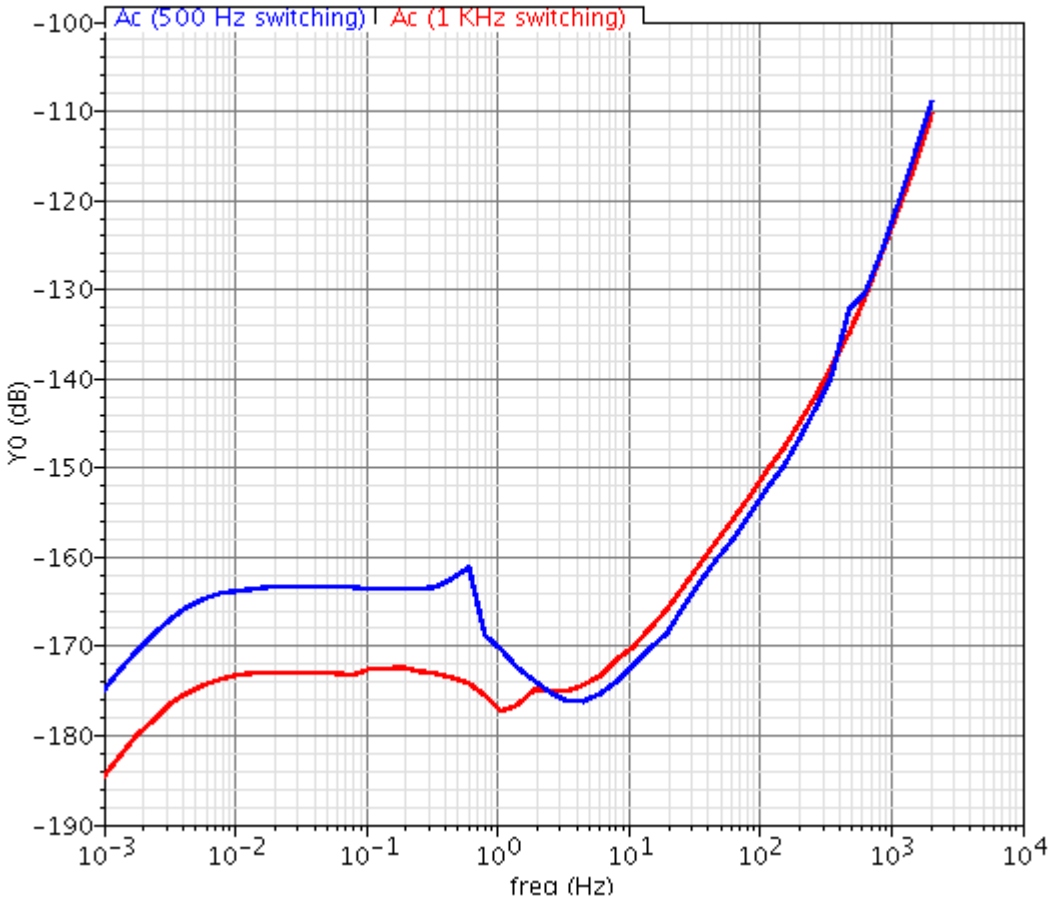

Figure 4-7 Common Mode Frequency Response

Fig 4-7 is a plot of the common mode gain of the INA with input clock frequencies of 500Hz and 1 kHz. The common mode gain for both cases is better than 160dB at mid-band frequencies. The CMRR of the amplifier is obtained by taking the ratio of the differential gain to the common mode gain and this is shown in Figure 4-8.

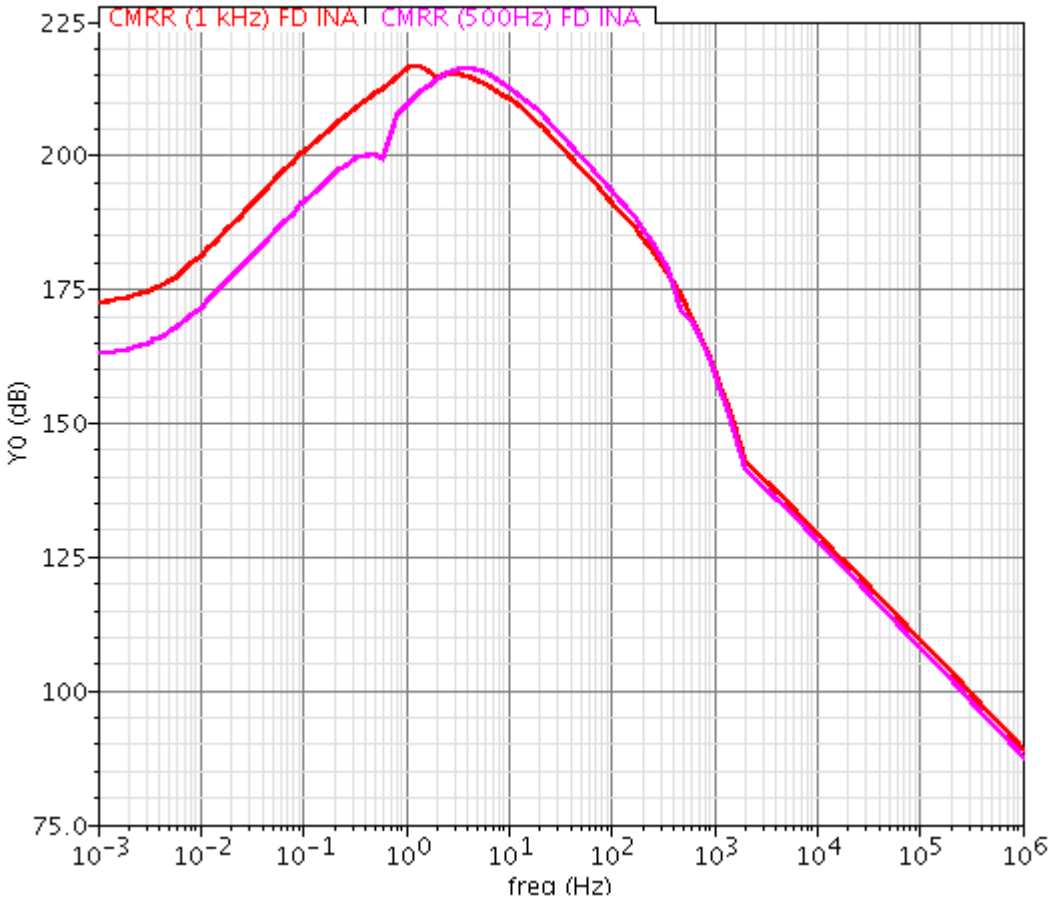

Figure 4-8 CMRR of Dynamically Matched Fully Differential INA

Examining the common mode gain curves shows that the Ac begins rise at 20dB per decade at the location of the HPF pole. This pole appears as a zero in the transfer function of common mode gain hence the degradation at that frequency.

4. Noise Performance

The noise performance of the INA is characterized using the input and output referred noise. Figure 4-9 shows this characteristic vs. frequency of the dynamically matched INA. Note that the input referred noise plot of the INA is very similar to the input referred noise of the opamp as was explained in previous sections. The integrated noise voltage of the INA between 0.5 Hz and 100 Hz is 3.015 $\mu V/\sqrt{Hz}$.

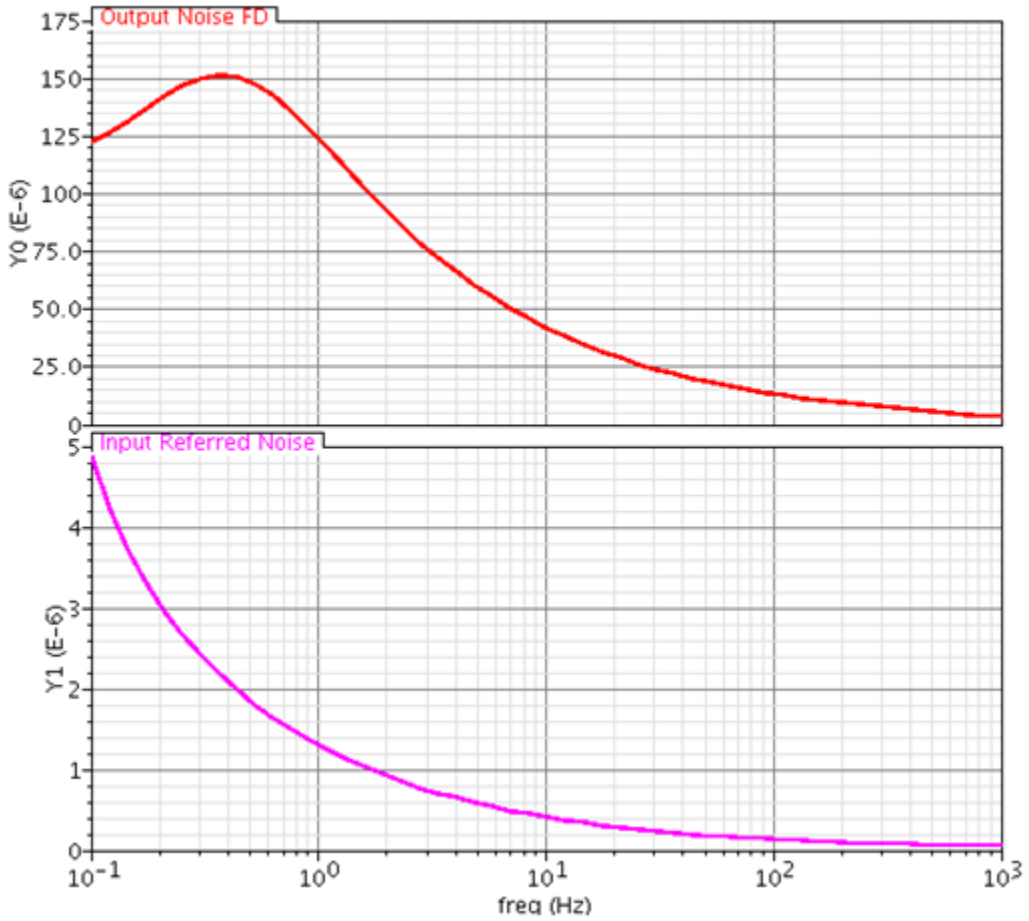

Figure 4-9 Output and Input Referred Noise of Dynamically Matched Fully Differential INA

5. Summary of Results Dynamically Matched Fully Differential INA

The power consumption, noise and CMRR performance of the fully differential INA are shown in Table 4-1. The simulated CMRR of the INA is 200 dB, an improvement of over 100dB over regular RC feedback INAs.

Table 4-1 Summary of Results - Dynamically Matched Fully Differential INA

Parameter	**Dynamically Matched Fully Differential INA**
CMRR (50 Hz)	200 dB
Gain	40 dB
Input Referred Noise	3.0 μV
Bandwidth	1 KHz
Power	19.4μW

C. Results – Dynamically Matched FBFS INA

1. Time Domain Signal

The time domain signals for the dynamically matched fully balanced fully symmetric INA are shown in Figure 4-10. The input signal to the INA is a 50Hz 2mV pk-pk signal. The voltages at the terminals of the feedback capacitors show the effect of capacitor swapping.

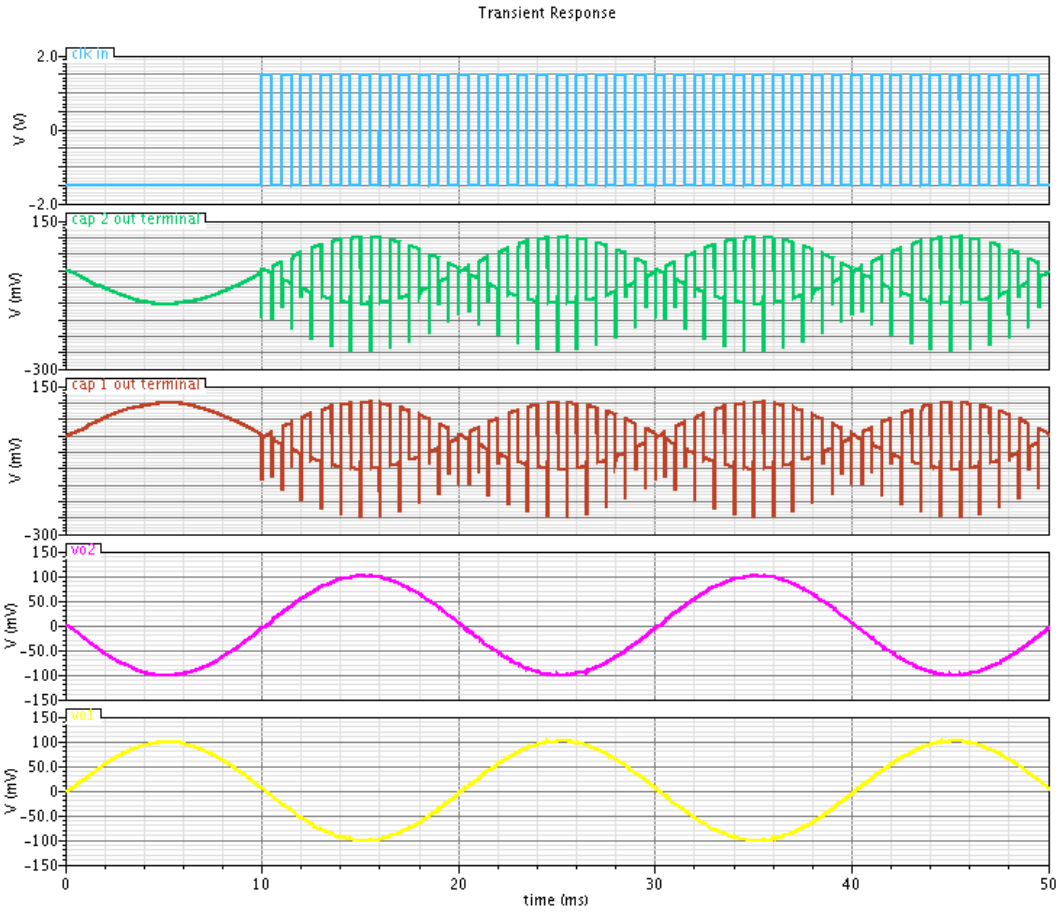

Figure 4-10 Transient Simulation of Dynamically Matched FBFS INA

2. Differential Mode Frequency Response

Figure 4-11 is the gain and phase response of the INA to differential input signals. The LPF is 800Hz while the HPF corner frequency is 0.4 Hz. Gain is 40dB at mid-band frequencies as is desired.

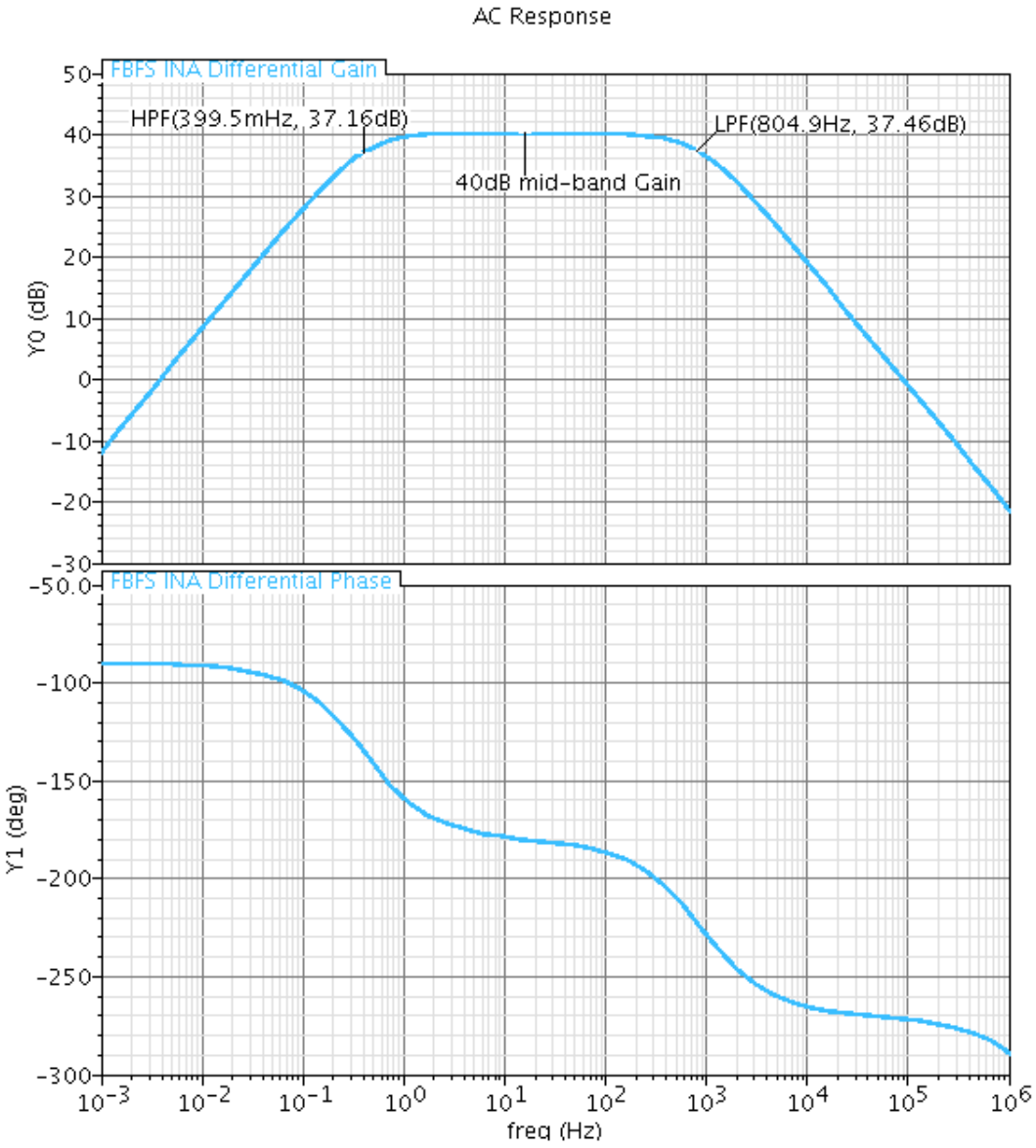

Figure 4-11 Magnitude and Phase of Dynamically Matched FBFS INA

3. Common Mode Frequency Response and Common Mode Rejection Ratio

Figure 4-12 is a plot of the common mode response of the INA. The common mode gain is better than 80 dB throughout the frequencies of interest. This is an improvement of over 40dB in common mode gain assuming 1% of capacitor mismatch.

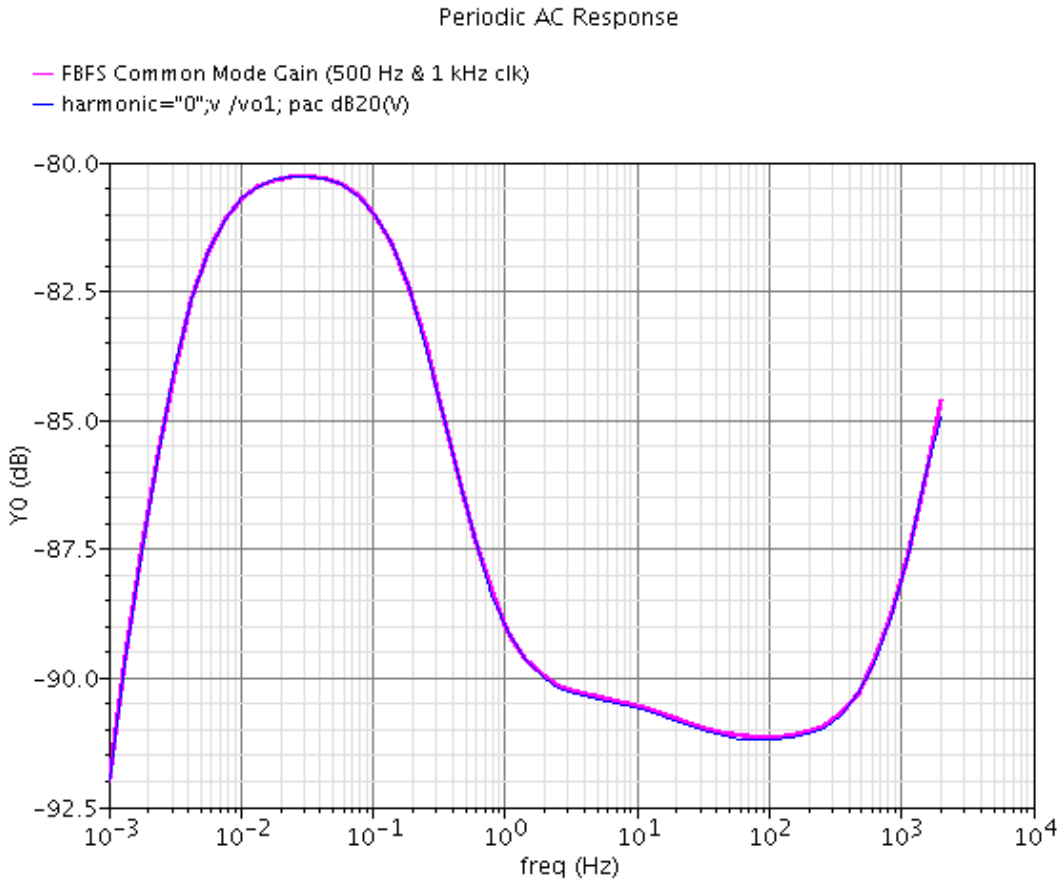

Figure 4-12 Common Mode Gain of Dynamically Matched FBFS INA

For the FBFS case, the common mode gain plots when the input clock frequency is 1kHz is exactly the same as when the clock switches at 500 Hz.

The CMRR response of the INA is shown in Figure 4-13. This plot is obtained by taking the ratio of the differential gain of the INA to the common mode gain. The improvement in CMRR over the conventional RC feedback INA is clear seen here. 130 dB of CMRR at mid-band frequencies is achieved here.

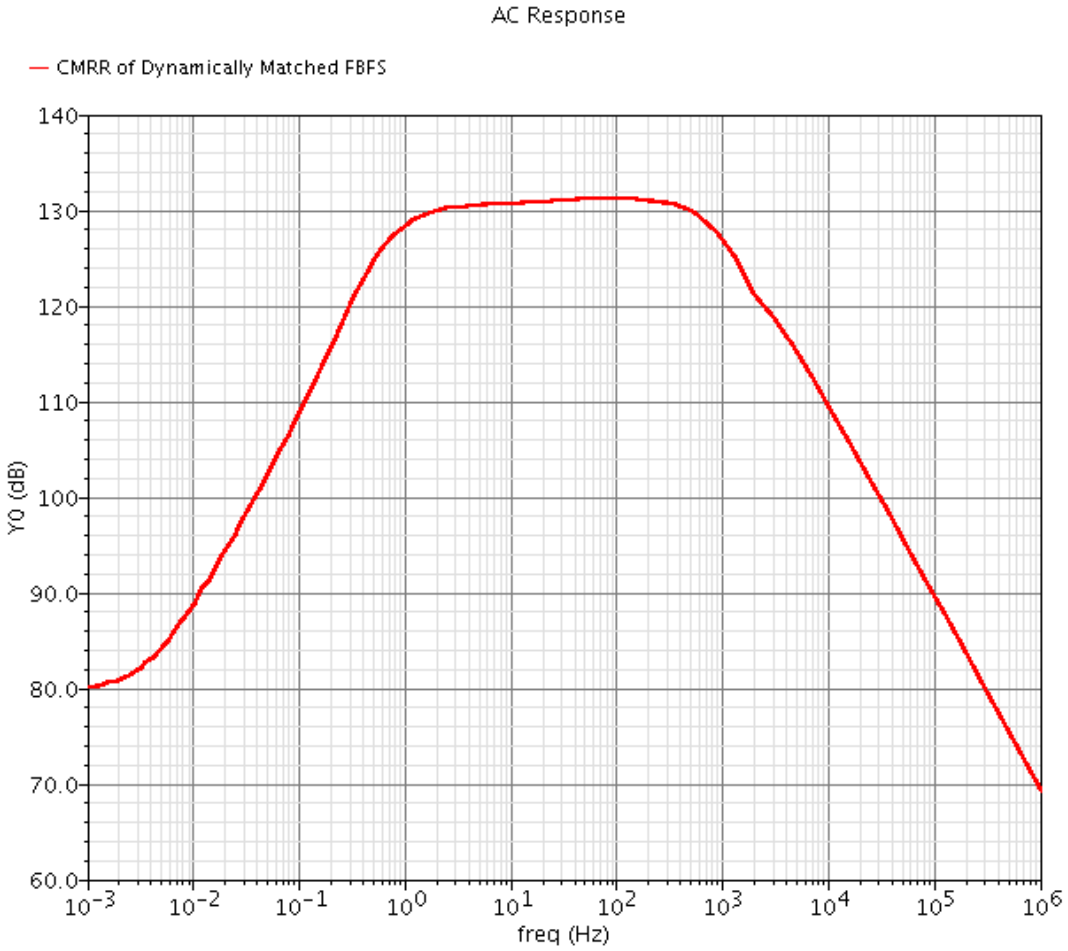

Figure 4-13 CMRR of Dynamically Matched FBFS INA

4. Input Referred Noise

The output noise and input referred noise of the dynamically matched fully balanced fully symmetric INA are shown in Figure 4-14. The response is similar to the fully differential INA response. However, the integrated noise between 1Hz and 100Hz referred to the input is 6.2 $\mu V/\sqrt{Hz}$.

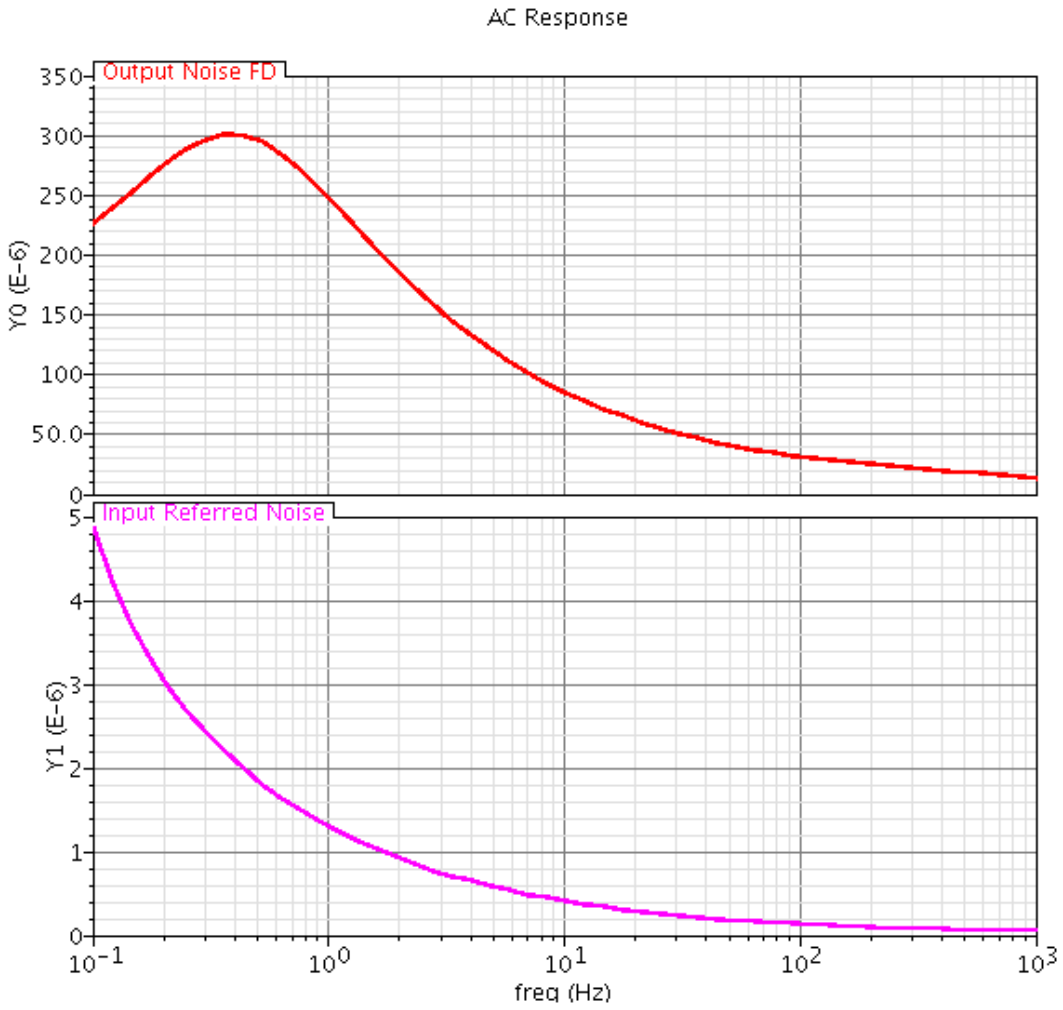

Figure 4-14 Output and Input Referred Noise of Dynamically Matched FBFS INA

5. Summary of Results Dynamically Matched FBFS INA

The power consumption, noise and CMRR performance of the fully balanced fully differential INA are shown in Table 4-2. The simulated CMRR of the INA is 130 dB, an improvement of over 50 dB over regular RC feedback INAs.

Table 4-2 Summary of Results - Dynamically Matched FBFS INA

Parameter	**Dynamically Matched FBFS INA**
CMRR (50 Hz)	130dB
Gain	40 dB
Input Referred Noise	6.0 μV
Bandwidth	800 Hz
Power	30 μW

5. SUMMARY AND CONCLUSION

Two instrumentation amplifiers have been proposed that utilize a dynamic element matching scheme to improve the CMRR (Common Mode Rejection Ratio) of INAs. The first INA is a fully differential INA based on a single fully differential opamp. The second is a fully balanced fully symmetric INA based on two individual single ended opamps. The proposed dynamic element matching technique greatly improves the CMRR of both INAs.

Table 5-1 is a summary of the results of this work in comparison to some other published works. It is clearly seen that the CMRR of the proposed amplifiers far exceeds the typical value for RC feedback INAs as in [1] and [7].

Table 5-1 Comparison of Results with Other Published Works

	[1]	**[9]**	**[3]**	**FD**	**FBFS**
Process	CMOS 1.5	CMOS 0.6	CMOS 0.6	CMOS 0.6	CMOS 0.6
INA Type	RC feedback	RC Feedback	Current Balancing	RC feedback	RC Feedback
CMRR	86 dB (mean)	71 dB	110 dB	200dB	130dB
Gain	40 dB	46 dB	68 dB	40 dB	40 dB
Referred Noise	2.4 μV	2.0 μV	60nV/Hz	3.0 μV	6.0 μV
Bandwidth	30 Hz	1 kHz	Variable	770 Hz	800 Hz
Power	0.64μW	1.75 mW	36μW	19.4μW	30μW

REFERENCES

[1] R. R. Harrison and C. Charles, "A low-power low-noise CMOS amplifier for neural recording applications," *IEEE Journal of Solid-State Circuits,* vol. 38, pp. 958-965, 2003.

[2] M. S. J. Steyaert and W. M. C. Sansen, "A micropower low-noise monolithic instrumentation amplifier for medical purposes," *IEEE Journal of Solid-State Circuits,* vol. 22, pp. 1163-1168, 1987.

[3] R. F. Yazicioglu, P. Merken, R. Puers, and C. Van Hoof, "A 60 uW 60nV/ Hz readout front-end for portable biopotential acquisition systems," *IEEE Journal of Solid-State Circuits,* vol. 42, pp. 1100-1110, 2007.

[4] C. V. H. Refet Firat Yazicioglu, Robert Puers, *Biopotential Readout Circuits for Portable Acquisistion Systems*, New York: Springer Publishing Company, Incorporated, 2008.

[5] J. H. Nagel, "Biopotential amplifiers," in *The Biomedical Engineering Handbook*, J. D. Bronzino, Ed., Boca Raton, Florida: CRC Press LLC, 2000

[6] J. G. Webster, "Biopotential amplifiers," in *Medical Instrumentation Application and Design*, 4th ed, M. R. Neuman, Ed, Boston: PWS Publishers, 1986.

[7] A. Bakker, K. Thiele, and J. H. Huijsing, "A CMOS nested-chopper instrumentation amplifier with 100-nV offset," *IEEE Journal of Solid-State Circuits,* vol. 35, pp. 1877-1883, 2000.

[8] C. C. Enz, E. A. Vittoz, and F. Krummenacher, "A CMOS chopper amplifier," *IEEE Journal of Solid-State Circuits,* vol. 22, pp. 335-342, 1987.

[9] R. R. Harrison, "A versatile integrated circuit for the acquisition of biopotentials," in *Proc. 2007 Custom Integrated Circuits Conference, 2007. CICC '07. IEEE*, pp. 115-122.

[10] S. Hongzhi, F. Deyou, J. Kemiao, F. Maarouf, Q. Hongwei, and X. Huikai, "A low-power low-noise dual-chopper amplifier for capacitive CMOS-MEMS accelerometers," *IEEE Sensors Journal,* vol. 11, pp. 925-933, 2011.

[11] T. Kugelstadt, "Getting the most out of your instrumentation amplifier design," *Analog Applications Journal,* 4th Quarther, pp 25-29, 2005.

[12] T. Delbruck and C. A. Mead, "Adaptive photoreceptor with wide dynamic range," in *Proc. 1994 Circuits and Systems, 1994. ISCAS '94., 1994 IEEE International Symposium on*, pp. 339-342 vol.4.

[13] C. Kok Lim, Z. Jianyu, and I. Galton, "Dynamic element matching to prevent nonlinear distortion from pulse-shape mismatches in high-resolution DACs," *IEEE Journal of Solid-State Circuits,* vol. 43, pp. 2067-2078, 2008.

[14] P. Rombouts and L. Weyten, "A study of dynamic element-matching techniques for 3-level unit elements," *IEEE Transactions on Circuits and Systems II: Analog and Digital Signal Processing,* vol. 47, pp. 1177-1187, 2000.

[15] E. A. Sobhy, S. Hoyos, and E. Sanchez-Sinencio, "High-PSRR low-power single supply OTA," *Electronics Letters,* vol. 46, pp. 337-338, 2010.

VITA

Name:	Reza Muhammad Abdullah
Address:	Texas A&M Department of Electrical Engineering, 214 Zachry, TAMU 3128, College Station, TX - 77843.
Email Address:	g3reza@tamu.com
Education:	B.Sc., Electrical Engineering, Kwame Nkrumah University of Science and Technology, 2008.